Wang *et al. Energy Mater* 2024;4:400050
DOI: 10.20517/energymater.2023.130

Energy Materials

Review

Open Access

Check for updates

Polymer-based electrolytes for high-voltage solid-state lithium batteries

Zixuan Wang[#], Jianxiong Chen[#], Jialong Fu, Zhiyong Li, Xin Guo[*]

School of Materials Science and Engineering, State Key Laboratory of Material Processing and Die & Mould Technology, Huazhong University of Science and Technology, Wuhan 430074, Hubei, China.
[#]Authors contributed equally.

***Correspondence to:** Prof. Xin Guo, School of Materials Science and Engineering, State Key Laboratory of Material Processing and Die & Mould Technology, Huazhong University of Science and Technology, 1037 Luoyu Road, Hongshan District, Wuhan 430074, Hubei, China. E-mail: xguo@hust.edu.cn

How to cite this article: Wang Z, Chen J, Fu J, Li Z, Guo X. Polymer-based electrolytes for high-voltage solid-state lithium batteries. *Energy Mater* 2024;4:400050. https://dx.doi.org/10.20517/energymater.2023.130

Received: 29 Dec 2023 **First Decision:** 2 Apr 2024 **Revised:** 24 Apr 2024 **Accepted:** 11 May 2024 **Published:** 23 May 2024

Academic Editor: Yuping Wu **Copy Editor:** Fangling Lan **Production Editor:** Fangling Lan

Abstract

Increasing the charging cut-off voltage of lithium batteries is a feasible method to enhance the energy density. However, when batteries operate at high voltages (> 4.3 V), the degradation of liquid organic carbonate electrolyte is accelerated and may cause safety hazards. Polymer-based electrolytes with inherently high safety and good electrochemical stability can prevent the electrolyte degradation in high-voltage solid-state lithium batteries. This paper provides a comprehensive and in-depth review of the design strategies, recent developments, and scientific challenges associated with polymer-based electrolytes for high-voltage applications. Emphases are placed on the interfacial compatibility between electrolytes and cathodes, such as mechanical contacts and interface chemical stability, which are critical to the lifespan of high-voltage lithium batteries. Moreover, guidelines for the future development of high-voltage solid-state lithium batteries are also discussed.

Keywords: Polymer-based electrolyte, interfacial compatibility, high-voltage stability, high energy density, lithium battery

INTRODUCTION

The current development of electric vehicles is constrained by various factors such as limited driving range, short battery lifespan, and slow charging speed, as outlined in previous studies[1]. The predominant focus for

addressing these challenges has been on enhancing the high-voltage tolerance of batteries. Polymer-based electrolytes stand out among various electrolytes due to their excellent processability, simple preparation procedures, and high safety[2,3]. However, these electrolytes in batteries are not universally applicable, as the strong oxidative/reductive nature of electrodes often challenges the realization of long-term, high energy density batteries[4,5]. Therefore, it is crucial to develop polymer-based electrolytes[6] with a wide electrochemical window and achieve compatibility between polymer electrolytes (PEs) and electrodes[7,8].

PEs can be classified into three categories: solid (SPEs), gel (GPEs) and composite PEs (CPEs) [Table 1]. In the 1880s, Wright and Fenton *et al.* initiated research on SPEs. The initial SPE matrix was polyethylene oxide (PEO), which could form ion-conductive polymers with electrical conductivity varying with temperature[9,10]. Lately, Vashisht and Armand applied polymers such as PEO and polyphenylene oxide (PPO) in solid-state batteries, introducing a new class of electrolytes, SPEs, which garnered attention[11]. However, SPEs exhibit a notable and critical flaw: notoriously low ionic conductivity that fails to meet practical application requirements[8,12]. Therefore, in 1975, Feuillade *et al.* added plasticizers to the polymer-salt system, in which the liquid content exceeded 20-30 wt.%, thereby introducing a new polymer system-GPEs[13-15]. GPEs combine the advantages of liquid and solid electrolytes. The liquid component exhibits excellent ion transport capacity and promotes good interface contact. It wets the gaps between electrode particles and between the electrode and the electrolyte, facilitating the formation of effective interfaces[16-18]. However, in order to adapt to the high-voltage cathode to achieve high-voltage lithium batteries, its electrochemical stability needs to be improved. In 1982, fillers were added to PEs for the first time to improve the mechanical properties and interface stability of the electrolytes[19]. For instance, Croce *et al.* employed nanoceramic powders as fillers to enhance the ionic conductivity of PEO-based PEs[20]. Subsequently, research on CPEs commenced. However, challenges such as the high cost of nanomaterials and difficulties in their dispersion in polymer matrices raised questions about the feasibility of industrial-scale application.

In recent years, researchers have conducted extensive studies on PEs, particularly focusing on the high-voltage performance, which is crucial for achieving high energy density in lithium batteries. The application of high-voltage PEs in lithium batteries must meet the following two criteria: (1) wide electrochemical window: > 4.3 V (*vs.* Li/Li^+), to match the high-voltage cathode material, so that it is not easily oxidized and decomposed at high potentials; and (2) Good interface compatibility: forming stable interfaces with the cathode and anode to ensure the normal operation of batteries and improve their performances.

This paper reviews the latest progress of polymer-based electrolytes for high-voltage lithium batteries [Table 2]. Combined with the selection of polymer functional monomers and electrolyte preparation strategies, the properties of PEs are customized. Importantly, this review not only provides insights into the high-voltage design of PEs but also emphasizes the significance of addressing the polymer electrolyte-electrode interfaces. It discusses effective approaches targeting the polymer electrolyte-electrode interfaces, combining our research progress in the field of polymer batteries with updated developments, focusing on the industrial scalability, cycling stability, and safety issues of polymer batteries.

HIGH-VOLTAGE POLYMER ELECTROLYTES

High-voltage solid polymer electrolytes

SPEs comprise lithium salts and polymer matrices, devoid of liquid solvents, exhibiting high safety, excellent mechanical properties, and good processability[2,3,21]. Among them, PEO stands out as the earliest studied and most widely applied SPE matrix of PEs. However, its poor oxidation stability limits its matching with the high-voltage cathode, mainly due to the unstable lone pair electrons of the ether oxygen atoms on the

Table 1. Comparison of various types of polymer electrolytes

Polymer electrolytes	Advantages	Disadvantages
Solid polymer electrolytes (SPEs)	Good mechanical properties	Low ionic conductivity Poor interfacial compatibility
Composite polymer electrolytes (CPEs)	Good ionic conductivity	Poor interfacial compatibility Difficult to disperse fillers
Gel polymer electrolytes (GPEs)	Good ionic conductivity Good interface contact	Poor mechanical strength

PEO chains[22-24]. Introducing antioxidant groups into polymer chains has proven effective in enhancing the high-voltage stability of polymer-based electrolytes. For instance, Yang *et al.* improved the electrochemical stability window (ESW) from 4.05 to 4.3 V by replacing the terminal group -OH of polyethylene glycol with a more stable -OCH_3 group[25]. This demonstrates that introducing strong antioxidant groups is an efficient strategy. To further demonstrate the impact of group substitution on ESW, Pandian *et al.* calculated the effect of substituent modification on PEO surfaces on ESW by density functional theory (DFT), as shown in Figure 1A[26]. CF_3 and CN functional groups have higher oxidation stability and can provide a wider ESW. Fluorination and cyano functional groups have been shown to have antioxidant properties[27].

Sun *et al.* introduced a strong electron-withdrawing trifluoroacetic acid group on poly-oxalate (POE), which enhanced the electronegativity of the highest occupied molecular orbital (HOMO), and the HOMO electrons were transferred to the oxalate center, thereby improving the oxidation stability[28]. Benefiting from this, the fluorine-terminated SPEs remained stable until voltages above 5 V, while the non-fluorine-terminated SPEs were oxidized at 4.8 V. Xie *et al.* further confirmed that the F atom transfers electrons to the middle of the polymer main chains, thereby preventing the decomposition and oxidation of the chains, and increasing the oxidation potential of the SPEs[29]. In addition to introducing fluorinated groups to improve the oxidation stability of the electrolytes, the formation of fluorinated crosslinked network structure not only improves the oxidation resistance of the electrolyte but also enhances the mechanical properties. Tang *et al.* also improved the oxidative stability of SPEs using a polyfluorinated crosslinking agent[30]. The SPEs exhibited good oxidation resistance through the multi-fluorinated segment induced electron-withdrawing effect and the constructed crosslinked network structure for electron effect transmission. The fluorinated SPEs can achieve a wide ESW of 5.08 V, as shown in Figure 1B. As demonstrated in Figure 1C, 2,2,3,3,4,4,5,5-diacrylate (OFHDODA) is the key to improving the electrochemical stability of SPE. The fluorine atoms with strong electron absorption properties can reduce the HOMOs and the lowest unoccupied molecular orbitals (LUMOs) of the fluorinated electrolytes, thus making the electrolytes show better oxidation resistance and reduction resistance.

In addition to the fluorine group, the strong electron-absorbing -C≡N group can also improve the oxidation stability of the electrolyte. Lv *et al.* prepared cyano-enhanced high-voltage SPEs by *in-situ* copolymerization of ethyl 2-cyanoacrylate (CA) and polyethylene glycol methyl acrylate (PEG)[31]. The SPEs form a stable interface layer rich in -C≡N and LiF on the surface of the $LiCoO_2$ (LCO) cathode, thereby improving the oxidation stability of ethylene oxide (EO) and inhibiting its decomposition. The wide ESW of the SPEs can reach 4.9 V [Figure 1D]. As shown in Figure 1E, the electrostatic potential of poly (CA-PEG) calculated by DFT shows that the negative electrostatic potential of -C≡N is much lower than that of EO segments, indicating strong interaction between the positive electrode and -C≡N, thus slowing the decomposition of EO segments. The team also synthesized rigid-flexible SPEs by crosslinking reaction of rigid poly (ethylene carbonate), flexible polyoxyethylene bis (amine) (POEA) and antioxidant aminopropionitrile (AN) without initiator. The preparation method and electrolyte characterization are shown in Figure 1F[32]. The polymer exhibits a wide ESW and excellent thermal stability. In summary, introducing antioxidant functional groups

Table 2. Progress of high-voltage polymer electrolytes

PEs	Polymer matrix	Liquid electrolyte	Preparation method	ESW (V)	σ (S cm^{-1})	t_+	Positive electrode	Voltage range (V)	Cycling lifespan (rate)	Ref.
SPE	C5-POE-F	LiTFSI/DMF	Solution casting	5	1×10^{-4}	-	NCM811	3.6-4.35	200 (0.15 C)	[28]
SPE	PVC/POEA/AN	LiODFB	Solution casting	4.6	4.47×10^{-5} (60 °C)	0.32 (60 °C)	LCO	3-4.3	150 (0.5 C, 60 °C)	[32]
SPE	PHMO	LiTFSI	Solution casting	4.6	1.26×10^{-4}	0.52	NCM811	3.0-4.3	250 (0.2 C)	[140]
SPE	PDADMAFSI	LiFSI/PYR13FSI	Solution casting	5.4	8×10^{-4}	0.44	NCM811	3-4.6	120 (0.1 mA cm^{-2})	[141]
SPE	PVDF-HFP/PAN/UiO-66-SO_3Li	LiTFSI/EMIMTFSI	Solution casting	5	7.5×10^{-4}	0.65	NCM811	3-4.3	150 (0.2 C)	[142]
SPE	PME/LiPVFM	LiTFSI/SN	Solution casting	5	3.57×10^{-4}	0.62	LCO	3-4.45	225 (0.5 C)	[143]
CPE	SiO_2/VEC	LiTFSI	Solution casting	5	1.35×10^{-3}	0.55	LCO	3-4.5	200 (0.1 C)	[48]
CPE	PEGDA/LLZO	LiDFOB/EC/DMC	Solution casting	5.13	1.25×10^{-3} (55 °C)	0.57	LCO	3-4.3	200 (0.2 C)	[57]
CPE	PEO-PVDF-HFP/LATP	LiTFSI/ACN	Solution casting	5.21	1.67×10^{-4}	0.49	NCM811	2.5-4.2	400 (0.5 C)	[144]
CPE	PVDF-HFP/Ce-NCATP	LiTFSI/DMF	Solution casting	5	2.16×10^{-3}	0.88	NCM811	3-4.3	200 (0.2 C)	[145]
CPE	PVDF/g-C_3N_4	LiFSI/DMF	Solution casting	4.7	6.9×10^{-4}	0.49	NCM811	2.5-4.3	1,700 (1 C)	[146]
CPE	PDOL/YSZ	$LiPF_6$/LiTFSI	Solution casting	4.9	2.75×10^{-4}	0.65	NCM622	2.8-4.3	800 (0.5 C)	[49]
GPE	PVDF/HEC	LiTFSI/PEGDME	Solution casting	5.25	7.8×10^{-4}	-	LNO	3.5-5	200 (0.2 C)	[147]
GPE	PAN@LAGP/PEGDA	LiTFSI/DMF	Solution casting	5	3.7×10^{-4}	-	NCM811	2.8-4.3	270 (0.5 C)	[148]
SPE	UFF/PEO/PAN	LiTFSI	Electrospinning	4.9	6.8×10^{-5}	0.5	NCM811	2.8-4.3	100 (0.35 mA cm^{-2})	[149]
CPE	γ-Al_2O_3-PPO	LiBOB-LiTFSI/NMP/SN	Electrospinning	5.6	3.38×10^{-4}	0.7	NCM622	2.8-4.3	120 (0.3 C)	[150]
GPE	PVDF-HFP/$BaTiO_3$	$LiPF_6$/EC/DMC	Electrospinning	5.1	5.2×10^{-3}	0.7	NCM532	2.5-4.5	200 (5 C)	[151]
SPE	CA-PEGMEA	LiFSI/SN/FEC	Thermal crosslinking	4.9	1.9×10^{-3}	0.56	NCM622	2.8-4.3	250 (0.1 C)	[152]
SPE	UPyMA/PEGDA	LiTFSI/NML	Thermal crosslinking	5.2	3.42×10^{-4} (20 °C)	0.66	LCO	3.0-4.6	1,000 (0.5 C)	[153]
SPE	CA-PEG/LLZTO	LiTFSI/Li DFOB	Thermal crosslinking	4.9	1.63×10^{-3} (30 °C)	0.4	LCO	3-4.5	100 (0.2 C)	[31]
SPE	PETEA	$LiPF_6$/FEC/FEMC/TFTFE	Thermal crosslinking	5.6	6.4×10^{-4}	0.48	LLO	2-4.8	200 (0.5 C)	[154]
SPE	P(VEC-co-TFEMA)	LiTFSI	Thermal crosslinking	5.7	5.02×10^{-5}	0.44	NCM811	3.0-4.5	300 (0.1 C)	[155]
SPE	PS/$Sn(Oct)_2$	LiTFSI	Thermal initiation	5	1.5×10^{-4}	0.78	LLO	2-4.6	100 (0.1 C)	[156]
GPE	MMA/TEGDMA/ETPTA	LiDFOB/FEC	Thermal crosslinking	5.65	2.24×10^{-4}	0.48	NCA	3-4.5	200 (0.2 C)	[64]
GPE	UPyMA/TEGDA	LiFSI/FEC/EMC/EGMEA	Thermal crosslinking	5.9	2.2×10^{-3}	0.75	NCM811	2.8-4.7	500 (0.5 C)	[157]
GPE	$LiNO_3$/DMAA	$LiPF_6$/EC/DEC/FEC	Thermal crosslinking	-	-	0.57	NCM622	3-4.3	400 (1 C)	[158]
GPE	DOL-PEE	LiTFSI/LiDFOB/FEC	Thermal crosslinking	4.5	2.36×10^{-3}	0.6	NCM622	-	300 (0.5 C)	[159]
GPE	TFEMA-PETA	LiTFSI/LiDFOB/FEC	Thermal crosslinking	4.89	1.88×10^{-3}	0.61	LCO	3-4.5	500 (1 C)	[160]
GPE	PEGDE-PEA	$LiPF_6$/DMC/FEC	Thermal crosslinking	4.8	7×10^{-4}	0.47	LCO	3-4.35	150 (0.2 C)	[161]

GPE	TFPO-PEE	LiDFOB/LiTFSI	Thermal crosslinking	5.1	3.98×10^{-3}	0.59	NCM622	4.5	300 (0.5 C)	[162]
GPE	ETPTA/SN	LiTFSI-LiDFOB/FEC	Thermal crosslinking	5.4	1.08×10^{-3}	0.64	LCO	3.0-4.3	300 (0.5 C)	[163]
GPE	PEGDA/PETA/PPO	$LiPF_6$/EMC/FEC	Thermal crosslinking	4.5	8.676×10^{-4}	0.65	NCM811	2.8-4.3	400 (1 C)	[164]
GPE	PMBA	LiTFSI-LiBOB/EC/EMC	Thermal crosslinking	5.64	1.385×10^{-3}	0.63	NCM622	3.0-4.3	700 (1 C)	[65]
GPE	DAP-PETEA	$LiPF_6$/FEC/FEMC/HTE	Thermal crosslinking	5.5	2×10^{-3}	0.43	LLO	2-5	200 (0.5 C)	[165]
SPE	PVC-TF3	LiTFSI/NMP	Thermal initiation	4.9	3×10^{-4} (60 °C)	0.76	NCM811	2.5-4.3	150 (0.1 C)	[166]
SPE	B-PEGMA/VC/AN	LiTFSI	Thermal initiation	5.1	9.24×10^{-4} (25 °C)	0.86	NCM811	2.8-4.3	100 (0.5 C)	[167]
GPE	PCUMA	LiDFOB/EC/DMC	Thermal initiation	5	1.27×10^{-3}	0.44	LCO	3-4.45	200 (0.5 C)	[168]
CPE	P(MVE-MA)	LiDFOB/PC	Thermal initiation	5.2	1.34×10^{-3}	0.54	LCO	2.75-4.45	700 (1 C, 60 °C)	[169]
CPE	LATP/PEO/PAN	LiTFSI/DMF	Thermal initiation	4.5	6.26×10^{-4} (60 °C)	0.82	NCM622	2.8-4.3	120 (0.5 C)	[170]
SPE	IL/OFHDODA/VEC	LiTFSI	UV	5.08	1.37×10^{-3}	0.4	NCM523	2.8-4.5	200 (0.5 C)	[30]
GPE	P(AMPSLi-MPEGA-AN)	$LiPF_6$/EC/PC	UV	5.06	2.5×10^{-3}	-	LCO	3-4.4	120 (0.2 C)	[66]
GPE	SN	LiTFSI/LiDFOB	Eutectic gels	4.8	1.87×10^{-3}	0.64	LCO	3-4.45	200 (1 C)	[171]

ESW: Electrochemical stability window; σ: ionic conductivity; t_+: ionic transference number.

is an effective method to enhance the oxidative potential of SPEs. Therefore, to design high-voltage-resistant SPEs, attention should be paid to selecting antioxidant groups, molecular structure design, and structural charge distribution. However, despite the excellent high-voltage stability exhibited by SPEs, their interface contacts limit their development, which will be discussed in detail in the following sections.

High-voltage composite polymer electrolytes

CPEs are composed of polymers, lithium salts and inorganic fillers, which have good processability and flexibility[33,34]. Inorganic fillers will adsorb trace water and impurities in polymers, improving the oxidation resistance of CPEs and increasing the electrochemical window[35,36]. According to the ionic conductivity of inorganic fillers, they can be classified into inert and active fillers. Commonly used inert fillers are silicon dioxide (SiO_2)[37-39], alumina (Al_2O_3)[40], titanium oxide (TiO_2)[41,42], magnesium oxide (MgO)[43], and zinc oxide (ZnO)[44]; active fillers are garnet type, NASICON type, and perovskite type[45]. Next, we will discuss the influence of different fillers on realizing high-voltage CPEs.

The inert fillers cannot conduct ions. When they form a crosslinked structure with the polymer matrix through physical/chemical interactions, the crystallinity of the polymer will be reduced, which is conducive to the ion transport. In addition, some chemical groups on the surfaces of the inert fillers have Lewis acid-base interaction with the anions/cations of lithium salts, which will promote the dissociation of the lithium salts and increase the number of free lithium ions, and this interaction improves the electrochemical stability of CPEs[46,47]. Wang *et al.* prepared size-adjustable antioxidant CPEs using a solution casting method, as shown in Figure 2A[48]. DFT calculations revealed the reasons for the increase in the antioxidant capacity of CPEs, as shown in Figure 2B. The area around

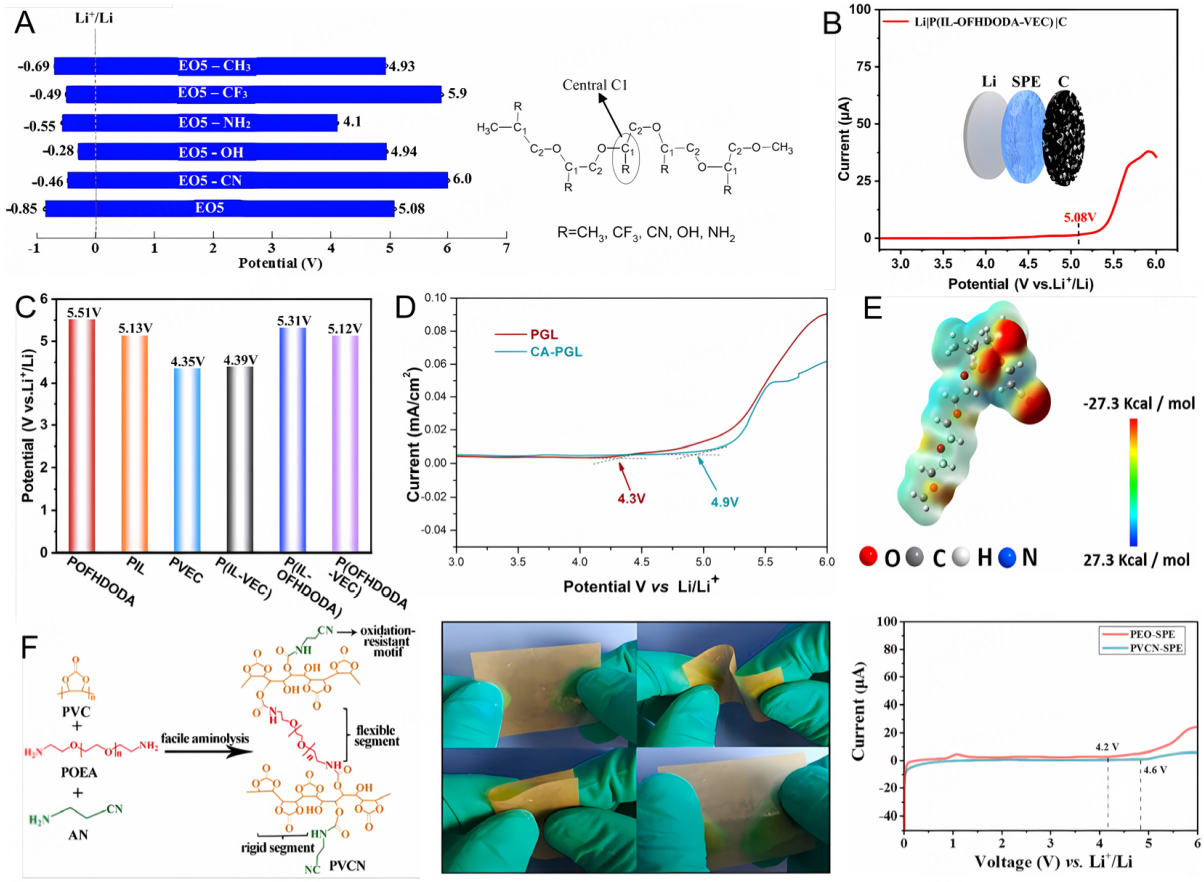

Figure 1. SPEs with antioxidant functional groups. (A) Effect of various functional groups (substituted at C_1 carbon) on the oxidation and reduction potentials (eV) of PEO (EO5) electrolyte. This figure is quoted with permission from Pandian *et al.*[26] Copyright 2018 American Chemical Society. (B) LSV curve of Li|P(IL-OFHDODA-VEC)|carbon. (C) ESW of PIL, POFHDODA, PVEC, P(IL-OFHDODA), P(IL-VEC), and P(OFHDODA-VEC). This figure is quoted with permission from Tang *et al.*[30] Copyright 2023 Royal Society of Chemistry. (D) LSV of PGL and CA-PGL at a scan rate of 0.5 mV s^{-1}.(E) Electrostatic potential of poly(CA-PEG). This figure is quoted with permission from Lv *et al.*[31] Copyright 2021 Royal Society of Chemistry. (F) Preparation diagram and characterization of PVCN-SPE.[32] Copyright 2022, Elsevier.

the O atom on the C=O group of poly(vinyl ethylene carbonate) (PVEC) and the O=S=O group of bis(trifluoromethylsulfonyl)imide ($TFSI^-$) has a high electron density, indicating that the O position of these groups in CPEs can preferentially form hydrogen bonds. Through the H atoms on the SiO_2 surfaces and the O atoms on the C=O and O=S=O groups in PVEC and TFSI, local intermolecular hydrogen bonding interactions can be formed. The local intermolecular interaction of hydrogen bonds in CPEs enhances the oxidation resistance, and its electrochemical window can reach 5 V [Figure 2C]. Inorganic fillers can also improve the ionic conductivity of PEs and enhance their electrochemical properties. Yang *et al.* introduced a Lewis acid filler yttrium stabilized zirconia (YSZ) and *in-situ* polymerization of 1,3-dioxolane (DOL) to increase the polymerization conversion of DOL monomers to 98.5%[49]. A large number of Lewis acid sites (oxygen vacancy, Zr^{4+} and Y^{3+}) on the YSZ surface can not only improve the degree of polymerization of DOL monomers, but also reduce the formation of by-products, thus improving high-voltage stability. As shown in Figure 2D, the leakage current of the PE remains very low at 4.9 V. The resulting solid electrolyte interface (SEI) is rich in Li_2ZrO_3 and its high ionic conductivity can guide the uniform deposition of lithium ions and delay the growth of lithium dendrites from the source [Figure 2E].

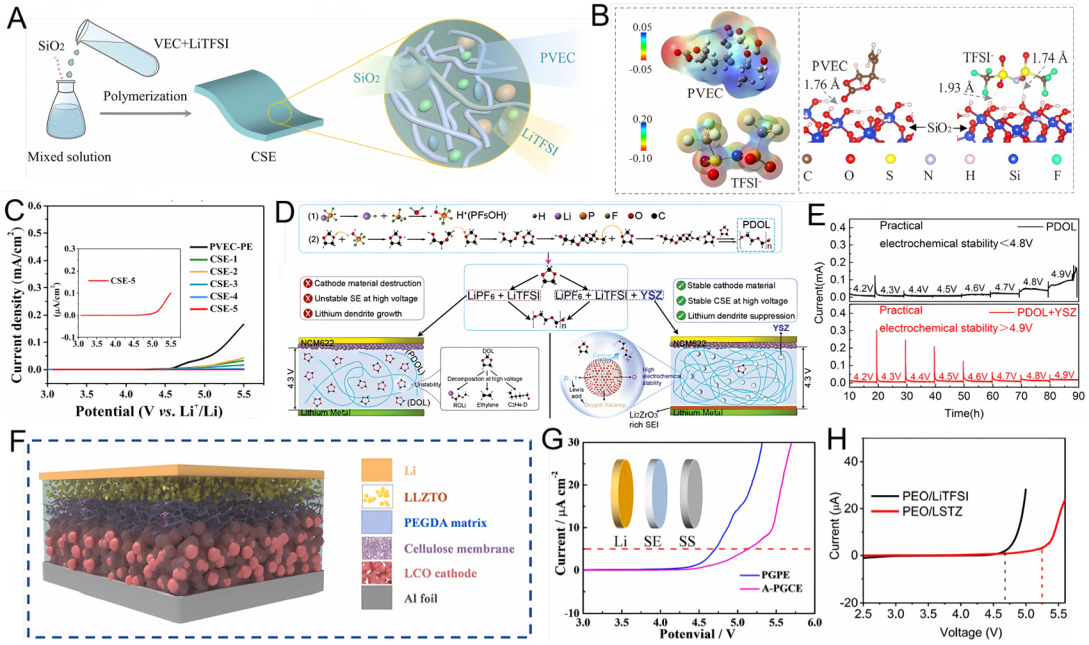

Figure 2. Fillers for improving the oxidation potential of CPEs. (A) Schematic diagram of preparing the CPE membrane from VEC precursor with Li salt and nanoparticles. (B) Molecular electrostatic potential energy mappings of PVEC and $TFSI^-$. And Intermolecular interaction in CPE by DFT calculation. (C) ESW of the as-involved electrolyte. This figure is quoted with permission from Wang *et al.*[48] Copyright 2022 Elevier. (D) Improving PDOL performance by YSZ. (E) Electrochemical floating analysis of cells assembled with NCM622 cathode for SE and CSE. This figure is quoted with permission from Yang *et al.*[49] Copyright 2022 Wiley. (F) Schematic illustration of *in-situ* fabricated LCO/electrolyte/Li cells. (G) Linear sweep voltammetry (LSV) curves of PGPE and A-PGCE. This figure is quoted with permission from Cai *et al.*[57] Copyright 2022 Elevier. (H) LSV curves of the PEO/LiTFSI and PEO/LSTZ electrolytes. This figure is quoted with permission from Xu *et al.*[59] Copyright 2019 National Academy of Sciences of the United States of America.

Compared to inert fillers, active fillers not only retain some characteristics of the inert fillers but also can directly participate in the transport of lithium ions, thereby further improving the electrochemical performance of the CPEs. Typical active fillers include oxide type (garnet type, perovskite type and NASICON type) and sulfide type fillers ($Li_{10}SnP_2S_{12}$ (LSnPS), $Li_{10}GeP_2S_{12}$ (LGPS), *etc.*)[50-52].

Garnet-type fillers are widely used in CPEs due to their high ionic conductivity, wide potential window (> 5 V *vs.* Li/Li^+) and good compatibility with lithium metal anodes[53-55]. Chio *et al.* added $Li_7La_3Zr_2O_{12}$ (LLZO) fillers to PEO, and the electrochemical stability increased with rising LLZO content. Thanks to the synergistic effect between organic matrix and LLZO, the ionic conductivity of SPEs has been greatly improved[56]. However, the inherent rigidity of inorganic solid electrolytes leads to poor electrolyte/electrode interface contact, which slows down the dynamics of charge and discharge, thus affecting the battery performance. Cai *et al.* introduced a small amount of $Li_{6.5}La_3Zr_{1.5}Ta_{0.5}O_{12}$ (LLZTO) nanoparticles into polyethylene glycol-diacrylate (PEGDA)-based GPE and prepared a novel asymmetric composite electrolyte with a LLZTO-rich layer by *in-situ* polymerization [Figure 2F][57]. The mechanically stable LLZTO layer induced uniform deposition of lithium and inhibited lithium dendrites, and its inherent high oxidation stability increased the decomposition potential of CPEs up to 5.13 V [Figure 2G].

Although the perovskite ceramic electrolyte has high ionic conductivity (10^{-3} S cm^{-1}) and high-voltage stability, it has poor compatibility with metallic lithium[58]. Xu *et al.* introduced $Li_{3/8}Sr_{7/16}Ta_{3/4}Zr_{1/4}O_3$ (LSTZ) perovskite that can also exist stably in a humid environment and used it as fillers to prepare a flexible PEO/lithium bis(trifluoromethylsulfonyl)imide (LiTFSI)/LSTZ solid composite electrolyte[59]. Ta^{5+} in LSTZ

formed a strong bond with F^- in $TFSI^-$ anions, which promoted the dissociation of lithium ions and improved the ionic conductivity of the electrolyte. The introduction of LSTZ also broadened the electrochemical window of the electrolyte [Figure 2H].

High-voltage gel polymer electrolytes

GPEs generally consist of a polymer matrix, a plasticizer and a lithium salt. The polymer matrix presents a crosslinked spatial network structure to provide a supporting skeleton, the plasticizer fills the structural gap, and the lithium salt and the polymer are dissolved in the plasticizer. They are a semi-solid electrolyte that improves the ionic conductivity while preventing the leakage of organic liquids. Their preparation methods mainly include *ex-situ* preparation and *in-situ* preparation[60]. The *ex-situ* preparation approach is to obtain GPEs and then assemble batteries, which leads to insufficient interface contact between electrodes and GPEs, resulting in an increase in resistance and a decline in the electrochemical performance of batteries[61,62].

The *in-situ* preparation method is to uniformly dissolve the polymer monomer, lithium salt, plasticizer and initiator into a liquid electrolyte, and then inject it into a battery cell to induce monomer polymerization under external conditions to form a GPE[60,63]. Here, we will mainly discuss the influence of *in-situ* preparation method on realizing high-voltage GPEs.

The *in-situ* polymerization of GPEs can be classified into thermal polymerization and photopolymerization. Thermal polymerization is a free radical polymerization initiated by heat treatment, which is cured at a corresponding temperature according to different types of initiators. Sun *et al.* explored the conductive mechanism of liquid electrolyte and GPE[64]. Lithium difluoro (oxalate) borate (LiDFOB) was dissolved in a fluoroethylene carbonate (FEC) solvent as a liquid electrolyte (FLE). Despite its high dielectric constant, FLE exhibits low ionic conductivity and poor electrochemical performance. F-GPE was synthesized by *in-situ* polymerization of methacrylate (MMA), triethylene glycol dimethacrylate (TEGDMA) and ethoxylated trimethylolpropane triacrylate (ETPTA) in FLE at 60 °C using azobisisobutyronitrile (AIBN) as an initiator, as shown in Figure 3A. Through molecular dynamics simulation, it is proved that F-GPE produces an electron-rich delocalized interface layer in the liquid phase and polymer matrix, providing a path for the lithium-ion migration, so that GPEs and lithium ions have higher binding energy, and the ionic conductivity is also improved. The ESW of the prepared F-GPE can reach 5.65 V, much higher than that of the liquid electrolyte. Chen *et al.* added 3 wt.% N,N′-methylenebisacrylamide (MBA) as a crosslinking agent into an alkaline liquid electrolyte, and AIBN as an initiator to obtain a quasi-solid electrolyte after *in-situ* thermal polymerization at 60 °C for 4 h[65]. They calculated the molecular orbital energy levels of each electrolyte component using the DFT to evaluate their redox activity. The molecular orbital energy of PAM-GPE and characterization are shown in Figure 3B. Among them, poly (N,N′-methylenebisacrylamide) (PMBA) has the LUMO energy level, indicating that it will be preferentially reduced on the lithium metal anode surface. At the same time, it also has the lowest HOMO, showing high oxidation resistance. This indicates that it is promising to block the electrolyte in the crosslinked structure of PMBA to prevent it from being decomposed under high voltages. The electrolyte was tested by linear sweep voltammetry (LSV). The results showed that the prepared PAM-GPE had an electrochemical stable voltage of 5.64 V, higher than 5.28 V of the liquid electrolyte. The thermal polymerization is carried out after the battery assembly is completed. This process is conducive to the full penetration of the electrolyte to form good interface contacts.

Photopolymerization is initiated through free radical polymerization under ultraviolet (UV) or gamma-ray irradiation, with light acting as the initiator. Zeng *et al.* synthesized a novel lithiated interpenetrating

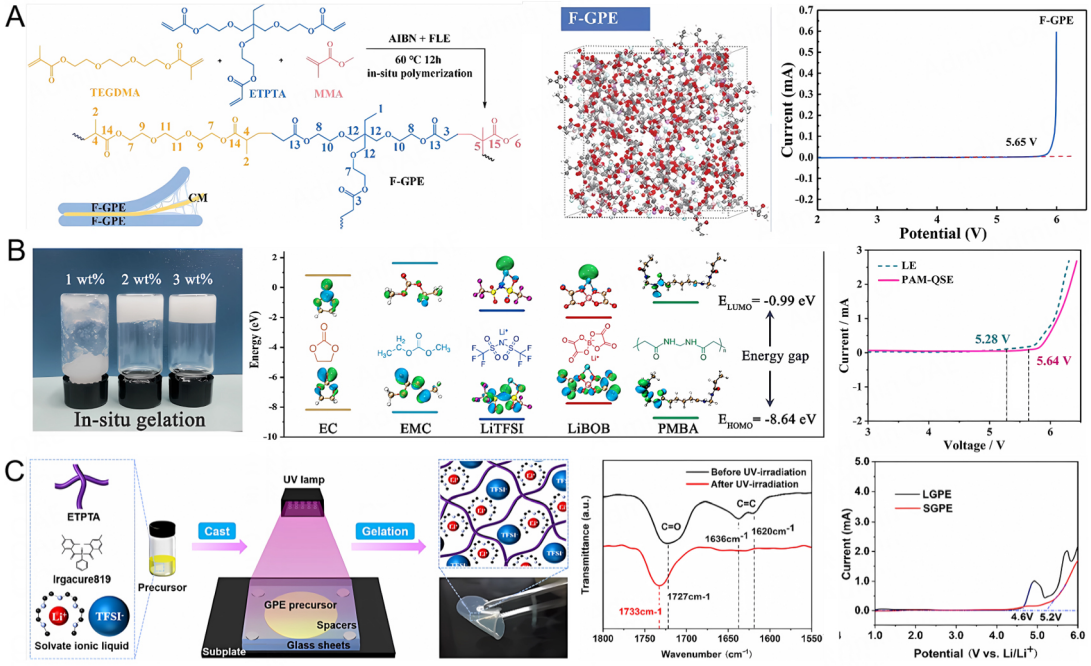

Figure 3. *In-situ* preparation of GPE. (A) Preparation and characterization of F-GPE. This figure is quoted with permission from Sun *et al.*[64] Copyright 2023 Wiley. (B) Molecular orbital energies and characterizations of PAM-QSE. This figure is quoted with permission from Chen *et al.*[65] Copyright 2021 American Chemical Society. (C) Preparation and characterization of SGPE. This figure is quoted with permission from Gao *et al.*[67] Copyright 2022 American Chemical Society.

network GPE by blending polyethylene glycol-acrylate (MPEGA), PEGDA, and AN in the presence of lithiated 2-acrylamido-2-methylpropanesulfonic acid, followed by two stages of UV irradiation polymerization[66]. This GPE has a wide electrochemical window of 5.06 V and good thermal stability (decomposition temperature of 400 °C). Nevertheless, the fabrication of the GPE involves two rounds of UV irradiation, leading to complex procedures and increased costs. Gao *et al.* realized a fast and efficient photocurable GPE using UV light to irradiate ETPTA and solvent-based ionic liquid for 30 s[67]. The preparation method and electrolyte characterization are shown in Figure 3C. The formed uniform silica gel-based GPE exhibits a wide electrochemical stable voltage of 5.2 V. Although photocuring can achieve rapid polymerization of materials, large-scale use of light radiation can cause harm to the human body and is costly.

In order to achieve high-voltage solid-state lithium batteries, it is not only necessary to focus on the high-voltage stability of the PEs, but also to consider the ionic conductivity, electrode and electrolyte compatibility, and the feasibility for achieving industrial development. Compared with SPEs and CPEs, the *in-situ* polymerization strategy of GPEs is more likely to be commercialized due to their good processability and flexibility and the high compatibility of the preparation process with the existing liquid battery technology. GPEs do not depend on conformational interfaces and, therefore, can adapt to the volume change of the electrodes during cycling. However, careful selection of the composition of GPEs is crucial, as the chemical composition of the interface ultimately determines the lifespan of batteries.

COMPATIBILITY OF POLYMER ELECTROLYTES WITH HIGH-VOLTAGE CATHODES

The design of high-voltage batteries also needs to consider the compatibility between PEs and electrodes, normally involving two main aspects: first, poor physical contacts at the cathode-electrolyte interface lead to

solid-solid contact deterioration (SPEs and CPEs). Following repeated lithium insertion/extraction cycles, the cathode undergoes phase transformation and surface reconstruction, leading to lattice mismatches and non-conformal contacts that result in high interfacial resistance[68]. This problem can be addressed through strategies such as electrolyte supplementation, deposition of external coatings, integration of electrode/electrolyte structures, and *in-situ* polymerization[69]. Another crucial aspect is the side reactions between the electrode material and the electrolyte, such as the decomposition of the electrolyte and the unstable cathode-electrolyte interface (CEI)/SEI due to the incompatibility between the electrolyte and the electrode[70,71]. The limited oxidative capability of the electrolyte leads to interface instability between the PE and the high-voltage cathode, causing inevitable electrolyte oxidation, degradation, and rapid capacity loss[72-74].

Interfacial physical contacts

As a critical battery component, the solid composite cathode directly determines the battery's output capacity and energy density[75,76]. However, there are compatibility challenges between high-voltage cathodes and conductive PEs[77]. Typically, porous electrodes with poor contact with the electrolyte exhibit discrete ion transport, exposing transition metal regions, which causes the electrolyte preferential decomposition into non-conductive interfaces, resulting in rapid capacity decay. This is due to the unevenness of the state of charge (SOC) within active particles and the loss of structural integrity at the sub-particle level[78], ultimately leading to sub-particle-level deactivation[79]. Conversely, cathodes with uniform contacts exhibit uniform particle-level SOC and high oxidation stability. The local microstructure of a high-loaded cathode is closely related to ion transport discreteness and capacity decay. In-depth understanding of the local structure and charge state of the cathode and their interaction with interface evolution can help achieve compatibility between the electrolyte and the cathode.

The ion transport discreteness in the cathode is influenced by its porosity. PEs have difficulty penetrating porous cathodes[80], leading to non-uniform distribution of local electric fields at heterogeneous contact points, reducing the electrochemical stability of batteries. Zhu *et al.* developed a liquid polymer electrolyte (LPE) composed of brush-like polymers with a main chain of polyphosphonitrile and a side chain of oligomeric EO[81]. LPE addresses issues such as electrolyte oxidation, poor lithium plating/stripping performance, and interface instability on the cathode. The flowable viscous LPE fully wets or even infiltrates the electrode to maintain good contact at the interface. $LiFePO_4$ and $Ni_{0.8}Co_{0.1}Mn_{0.1}O_2$ (NCM811) batteries using this LPE achieve long-term stable cycling in the temperature range of 60 to 120 °C, with a Coulombic efficiency of about 100%. Increasing the surface coverage of the electrolyte and improving the inherent stability of the electrolyte are expected to achieve a stable interface. An *et al.* designed a high-loaded composite cathode (12 and 28.6 mg cm^{-2}) with a fully active surface through a solvent-free *in-situ* liquid-solid conversion strategy[82]. As shown in Figure 4A, the dual modifications through physical structure reshaping and chemical methods enable high-loaded NCM811 batteries to exhibit an excellent lifespan exceeding 10,000 h and over 150 cycles with a cathode loading of 28.6 mg cm^{-2}.

Additionally, a cathode normally undergoes volume changes during the cycling process, while the deformability and wetting properties of the solid electrolyte are poor, which leads to interface gaps[83]. Therefore, achieving a flexible interface between the electrolyte and the electrode is crucial. Wang *et al.* utilized poly(acrylonitrile-butadiene) (PAB) polymer as a coating for $LiNi_{0.6}Mn_{0.2}Co_{0.2}O_2$ cathode material, as depicted in Figure 4B[84]. The PAB nano-soft layer can enhance the physical contact between the cathode and the solid electrolyte. Coupling the cathode with lithium metal and poly(ethylene-acrylic ester) (PEA) solid electrolyte, the solid-state battery exhibited excellent rate performance (99 mAh g^{-1} at 3 C) and good cycling stability (75% capacity retention after 400 cycles). Quasi-solid or gel polymer electrolytes (QSEs or GPEs) containing organic small molecule plasticizers/solvents are expected to improve interface contacts[74]

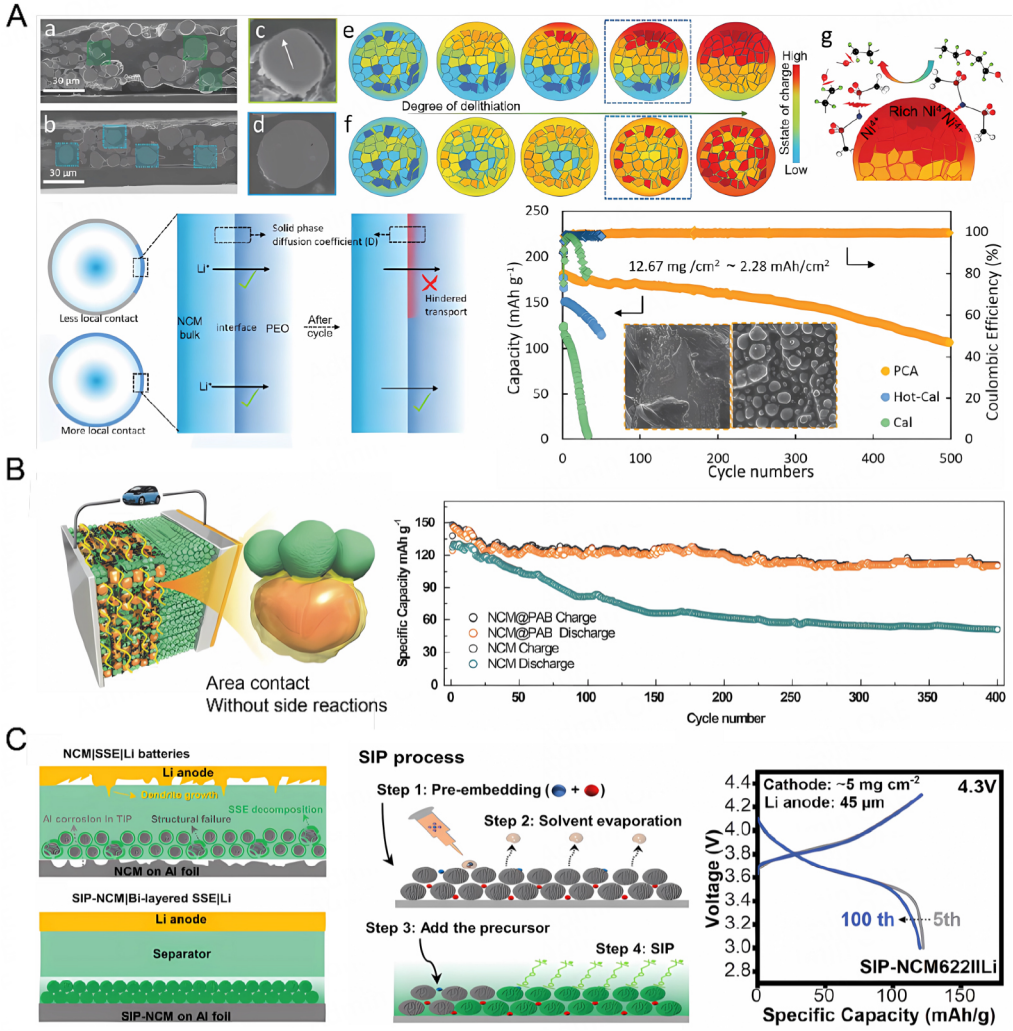

Figure 4. The mechanical contact between polymer-based electrolytes and electrodes. (A) High state of charge in particle scale at local contact accelerates the decomposition of electrolyte. This figure is quoted with permission from An *et al.*[82]. Copyright 2023 Wiley. (B) Schematic representation and electrochemical performance of solid-state batteries. This figure is quoted with permission from Wang *et al.*[84] Copyright 2018 Wiley. (C) Interface optimization between SIP-derived coating and cathode, along with the enhanced cycling performance of NCM622||Li cell under high voltage conditions. This figure is quoted with permission from Chen *et al.*[87] Copyright 2023 Wiley.

and room temperature ionic conductivity[85,86]. Surface *in-situ* polymerization (SIP) with optimized interface interactions can enhance interface compatibility between various cathodes and PEs, offering the potential for enduring high-voltage tolerance. Chen *et al.* achieved durable and tunable SPEs on the cathode side through *in-situ* polymerization of a polymerizable ether-based electrolyte (SIP), as illustrated in Figure 4C[87]. SIP involvement in constructing a homogeneous polyether/LiTFSI coating can optimize the interface interactions between the PE and the $LiNi_xCo_yMn_zO_2$ (NCM, $x + y + z = 1$, $x \geq 0.8$) cathode. Additionally, its derived ultra-thin CEI-like coating can provide close/conformal contact between the cathode and the electrolyte. The assembled NCM811||Li full cell achieved super-stable cycling performance and high Coulombic efficiency.

Interfacial chemical reactions

The working potential of the high-voltage cathode exceeds 4 V; the practical operation of lithium batteries is constrained by the oxidative nature of the cathode[88,89]. Intense oxidation of transition metals and irreversible loss of lattice oxygen at high charge states lead to electrolyte decomposition and reduced conductivity at the cathode-electrolyte interface[90]. Molecular structure design can enhance the antioxidant properties of PEs, aiding in constructing a stable CEI[91]. Copolymerization of multiple monomers can compensate for the limitations of individual polymers, widening the ESW. This is a critical requirement for the compatibility of PEs with high-voltage cathode materials. However, PEs containing easily oxidizable oxygen-containing groups typically exhibit narrow ESW, resulting in poor cycling stability under high potentials. Conversely, widening of the ESW up to 4.8 V can be achieved by ring-opening polymerization of oxidizable cyclic carbonates using organic metal catalysts[92]. Additionally, it is noteworthy that strong electron-withdrawing groups can further enhance the antioxidant properties of the polymer matrix[93], as previously discussed. Solid electrolytes possess stronger dendrite suppression capabilities than liquid electrolytes, offering potential for applications in high-capacity lithium metal anodes[94]. However, due to the accumulation of interface voids and volume changes during repeated lithium stripping processes, contact losses between solid electrolytes and electrodes result in large ion transport barriers, deteriorating the electrochemical performance of solid-state lithium metal batteries[95].

Constructing functional interfaces[92] and electrode modifications[96] can achieve compatibility between PEs and electrodes, where the interface components and structural characteristics directly influence the rapid transmission of lithium ions. Metal-organic frameworks (MOFs), due to their high surface area, structural stability, tunable porosity, and abundance of Lewis acid sites, have been utilized for electrode interface modification or as electrolyte fillers to enhance ion transport and charge transfer processes, thereby suppressing lithium dendrite formation[97]. Qian *et al.* reported a porous and robust MOF coating (MOF-199), where the sturdy MOF interfacial layer physically inhibits lithium dendrite growth[98]. Its highly polar structure promotes uniform Li^+ concentration, thereby mitigating excessive SEI formation. Lithium metal batteries protected by MOF-coating achieved 97% Coulombic efficiency at a current density of 1.0 mA cm^{-2}. Huo *et al.* employed cationic MOFs (CMOFs) to immobilize anions and guide uniform Li^+ deposition, enabling dendrite-free solid-state batteries[99]. CMOFs, through electrostatic interactions with charge carriers and their high surface area, securely bind anions, enhancing the transference number of Li^+ to 0.72[99]. Furthermore, customization with CMOFs grafted with -NH_2^+ groups can protect the polymer chain's ether oxygen via hydrogen bonding, widening the ESW to 4.97 V. Cui *et al.* achieved excellent lithium-ion transport and interface stability by utilizing a MOF layer and atomic layer deposition of Al_2O_3 at the modified polymer matrix interface[100]. The inert Al_2O_3 nano-coating enhances affinity with the lithium negative electrode and participates in forming the SEI film, reducing the diffusion barrier for lithium ions. After 500 cycles within a wide voltage range of 2.0-4.8 V, the capacity retention remained at 84.6%. Inorganic coatings can improve the electrochemical stability of the interface; however, they often involve intricate processing steps and high stiffness, making it challenging to accommodate the volume changes of the cathode during charge/discharge cycles. *In-situ* formation of a homogeneous electrode/electrolyte interface layer via electrochemical methods, using highly flexible polymers, can simultaneously mitigate cathode-electrolyte side reactions and enhance contacts at the solid-solid interface during the cycling process. Ma *et al.* performed UV-curing of FEC and triethyl phosphate (TEP) carbonate-based precursors separately on two electrodes, developing a dual-function polymer electrolyte (BDFPE) with low interfacial resistance [Figure 5A][101]. The functional additives FEC and TEP have low LUMO and high HOMO, aiding in interface formation[46]. Regulation of the electrolyte molecular structure and additive composition can achieve compatibility between the electrolyte and high-voltage cathodes, such as fluorination and nitrogenation[102]. The solid electrolyte adheres closely to the lithium metal anode and the nickel-rich cathode, facilitating continuous lithium flux and avoiding large interface transfer barriers between the

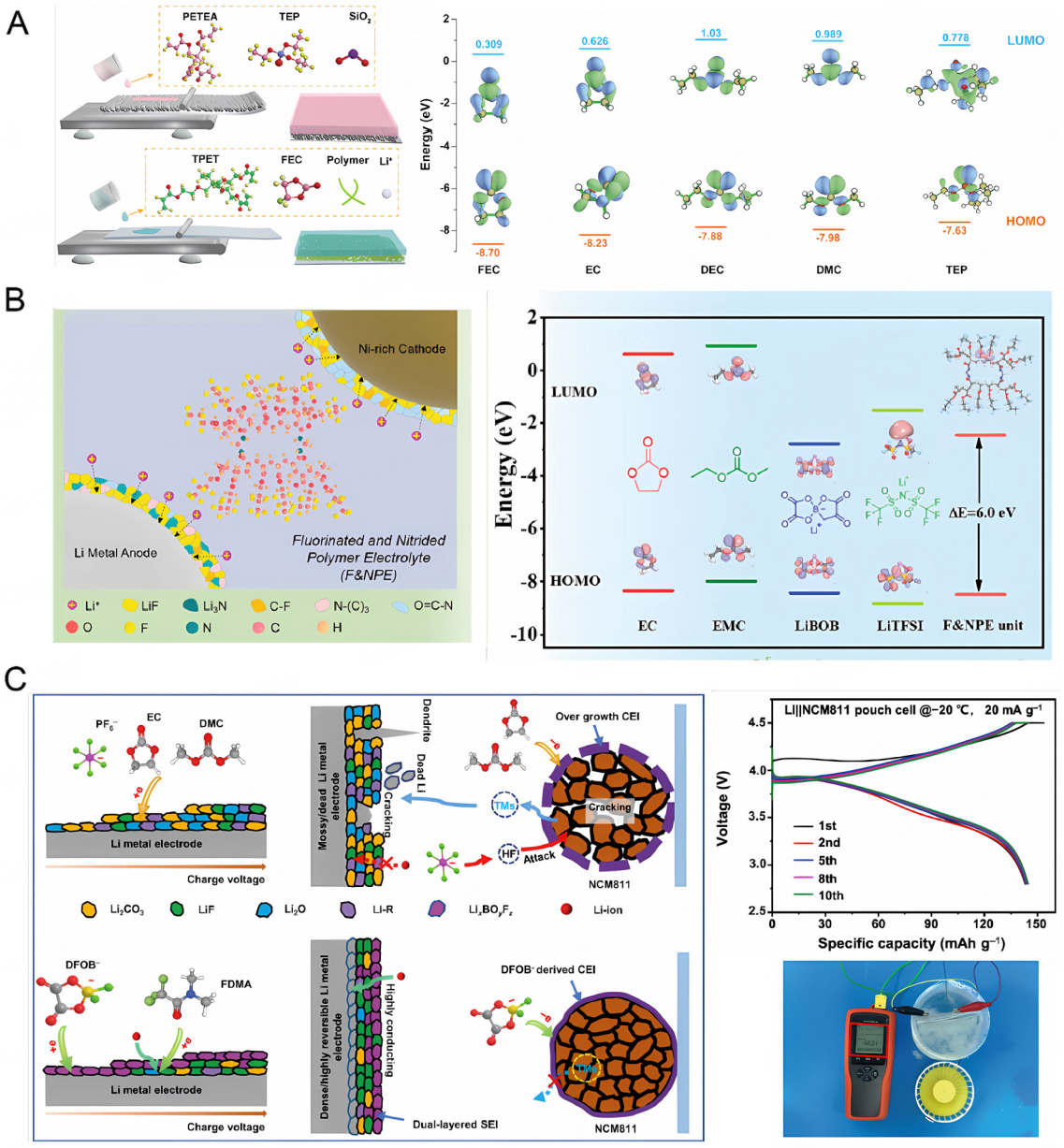

Figure 5. Interface chemistry between polymer electrolytes and electrodes. (A) Preparation of bidirectional functional polymer electrolytes and their assembled battery performance. This figure is quoted with permission from Ma *et al.*[101]. Copyright 2023 Wiley. (B) Stable interface design for NCM622/F&NPE/Li batteries and cycling performance of NCM622//Li batteries. This figure is quoted with permission from Qi *et al.*[103] Copyright 2023 Wiley. (C) Solid electrolyte interface formed on lithium metal electrodes and electrochemical performance of batteries. This figure is quoted with permission from Li *et al.*[107]. Copyright 2023 Springer Nature.

electrode and electrolyte. Benefiting from the BDFPE design, Li||Li symmetric cells achieved smooth and dendrite-free lithium deposition after an extended 1,800 h of cycling at 1 mA cm^{-2}. Qi *et al.* reported fluorinated and nitrided polymer electrolytes (F&NPE) composed of 2,2,3,4,4,4-hexafluorobutyl acrylate (HFBA) and N,N′-methylenebisacrylamide (MBAM), as depicted in Figure 5B[103]. Based on molecular-level design of the PE, robust CEI and SEI were simultaneously constructed. The lithium-affinitive N-$(C)_3$ in the SEI guided uniform distribution of Li^+, promoting the transport of Li^+ through LiF and Li_3N for uniform Li^+ deposition and stripping. Additionally, antioxidative fluorination and nitrogenation moieties in the CEI

suppressed parasitic reactions between the cathode and electrolyte and structural degradation of the cathode. Therefore, NCM622/F&NPE/Li cells exhibited an 85.0% capacity retention after 500 cycles at 4.5 V voltage and 0.5 C.

In-situ polymerization with liquid monomers, similar to conventional liquid electrolytes, exhibits excellent wetting properties. Therefore, it can permeate electrodes to achieve sufficient contact with the active material, enabling close interaction between electrodes and PEs[3,104]. Lithium batteries face challenges in cold climates due to insufficient dynamics in the electrolyte itself and at the electrode/electrolyte interfaces. At low temperatures, inadequate ion and charge transport dynamics in the electrolyte and at the electrode/electrolyte interface can lead to structural changes at the SEI[105,106]. Li *et al*. reported a PE, polyoxymethylene (POM), prepared by *in-situ* polymerization using the precursor 1,3,5-trioxane[107]. POM has a wide bandgap and can stabilize the NCM811 cathode at high voltages (e.g., > 4.4 V)[108]. PEs can form a dual-layer SEI on the lithium metal anode [Figure 5C], consisting of an amorphous $Li_xBO_yF_z$ outer layer and an inner layer rich in LiF. $Li_xBO_yF_z$ and LiF are excellent electron insulators with a large electrochemical window, suppressing electrolyte decomposition and dendrite formation[109]. The amorphous $Li_xBO_yF_z$ is highly plastic, mechanically adapting to the volume changes of the electrode[110].

COMPATIBILITY OF POLYMER-BASED ELECTROLYTES WITH OTHER NEGATIVE ELECTRODES

The formation of a stable SEI layer on negative electrodes is crucial for extending the lifespan and maintaining high capacity in lithium-ion batteries (LIBs)[111]. The ideal physical thickness of a SEI layer is on the order of a few angstroms (Å), with high mechanical strength to accommodate volume expansion and contraction during charge and discharge processes[112]. Graphite is a common negative electrode material for LIBs, and the formation of its surface SEI layer is influenced by graphite type, electrolyte composition, electrochemical conditions, and temperature. The slow electrochemical processes on the graphite surface limit the fast charging performance of LIBs, including lithium desolvation in the SEI and lithium transport in the SEI[113]. Additionally, graphite's low equilibrium potential (~0.1 V *vs.* Li/Li^+) results in a low overpotential capacity limit, forming metallic lithium when the anode potential drops below 0 V (*vs.* Li/Li^+), leading to poor cycle stability and even safety issues. SEI composition and structure are crucial in modulating the lithium desolvation structure at the negative electrode interface and accelerating the rapid charging process of LIBs. Electrolyte additives, high-concentration electrolytes, and graphite surface coatings contribute to forming a stable SEI, preventing further electrolyte decomposition[114]. The electronic resistance increases the potential of the graphite surface and shifts the negative electrode surface potential in the stable window of the electrolyte. The electronic insulation and compact structure of the SEI prevent continuous reduction of the anode surface by the electrolyte and the intrusion of solvents into the SEI, embedding further into bulk graphite.

The specific capacity of silicon (Si) negative electrodes is ten times that of traditional graphite anodes (372 mAh g^{-1})[115]. However, the alloying/dealloying reactions between Si and Li cause significant volume changes, leading to severe anisotropic stress and particle fragmentation[116]. Furthermore, volume changes result in continuous variation of the SEI interface, rapidly depleting electrolyte and lithium ions. Unique nanostructures (nanowires, nanotubes, core/shell structures, nanoporous materials, *etc.*) and composites using electrochemically inert/low-active materials (such as carbon, conductive polymers, *etc.*) can reduce internal stresses and leverage their supporting structure, large specific surface area, and short lithium diffusion length to enhance their cycling lifespan. Nevertheless, limitations in volumetric energy density and reduced mass loading on electrodes will restrict industrial applications. It is noteworthy that silicon and graphite can be processed using the same commercial production lines, enabling high manufacturability

and low investment. Si/graphite/C composite material designs contribute to enhancing negative electrode capacity and structural stability[117], thereby reducing battery pack and manufacturing costs.

GAS GENERATION IN HIGH-VOLTAGE LITHIUM BATTERIES

The highly lithiated surfaces of the cathode/anode during charging/discharging processes in high-voltage lithium batteries lead to gas generation upon oxidation/reduction. Gas evolution in the battery due to swelling results in capacity decay, increased impedance, loss of cell integrity, and poses new safety risks[118]. Therefore, controlling gas generation in the cathode, anode, and electrolyte is crucial for the safe and high-performance operation of batteries.

High-voltage cathode materials are key to achieving high energy density in lithium batteries; however, the cathode side is often a significant source of battery gases. For instance, layered materials [Figure 6A], such as Li_xMO_2, Li_xNiO_2 (LNO), and Li_xMnO_3 (LMO) ($x < 1$), are metastable kinetically and undergo oxygen activation at high voltages, leading to oxygen release[119]. Similarly, LCO undergoes irreversible phase transition to CoO_2 via spinel and rock-salt structures during over-oxidation, releasing O_2. Subsequently, CoO_2 undergoes further oxidation, resulting in oxygen loss. Over-delithiation of the cathode generates heat and releases O_2, which, in turn, accelerates electrolyte decomposition[120,121]. For instance, layered transition metal oxide cathodes can react with carbonate-based solvents [e.g., propylene carbonate (PC), ethylene carbonate (EMC), ethyl methyl carbonate (EMC), diethyl carbonate (DEC), and dimethyl carbonate (DMC)] in QSEs to produce CO_2[122,123]. Ring-structured solvents are prone to ring-opening reactions and decomposition; thus, selecting chain-structured carbonates in the GPE reduces gas evolution.

Chemical reactions at the interface between the cathode and electrolyte are the primary sources of gas generation in batteries. For instance, when charging voltage exceeds 4.5 V, the escape of $^1O_2$ from $LiNi_xMn_yCo_zO_2$ (NMC) lattices leads to further oxygen release. Additionally, cathode contaminants, such as lithium carbonate (Li_2CO_3), often appear on the cathode surface during NMC or lithium-rich manganese-based layered cathode material preparation and storage[124]. Under a relatively low voltage of 3.8 V, the decomposition reaction $2Li_2CO_3 \rightarrow 4Li^+ + 4e^- + 2CO_2 + {}^1O_2$ occurs, and at high voltages, $^1O_2$ reacts vigorously with the electrolyte, further producing gases such as CO_2 and CO[125]. Two typical ternary nickel-rich layered cathode materials, NCM and $LiNi_xCo_yAl_zO_2$ (NCA, $x + y + z = 1$, $x \geq 0.8$), generate CO and CO_2 gases at their surfaces through (i) electrochemical oxidation; and (ii) chemical oxidation[126]. As illustrated in Figure 6B, electrochemical oxidation at the cathode surface occurs at voltages higher than electrolyte decomposition[126]. For example, EC oxidation at the positive electrode interface produces CO, CO_2, and protons ($R\text{-}H^+$), leading to electrolyte degradation; subsequently, proton reduction at the negative electrode produces H_2. Conversely, phase transitions in layered NCM structures and the release of highly active singlet oxygen ($^1O_2$) lead to chemical oxidation of EC, resulting in CO_2, CO, and H_2O. Higher nickel content facilitates lattice oxygen oxidation, with oxygen being released after a decrease in oxygen binding strength[127]. Additionally, surface restructuring of nickel metal ions (e.g., $LiMO_2 \rightarrow MO + \frac{1}{2}O_2$) contributes to increased oxygen release[128].

PEs can widen the ESW of the electrolyte by crosslinking structures or grafting high-voltage-resistant groups, effectively suppressing electrochemical oxidation of the electrolyte and reducing gas evolution from layered transition metal oxide cathodes under high voltages.

The escape of negative electrode gases at low potentials is crucial for achieving high performance in LIBs[129]. Due to the absence of a stable SEI on the negative electrode surface during the initial cycles of battery operation[130], electrolyte components on the negative electrode side are prone to generating highly

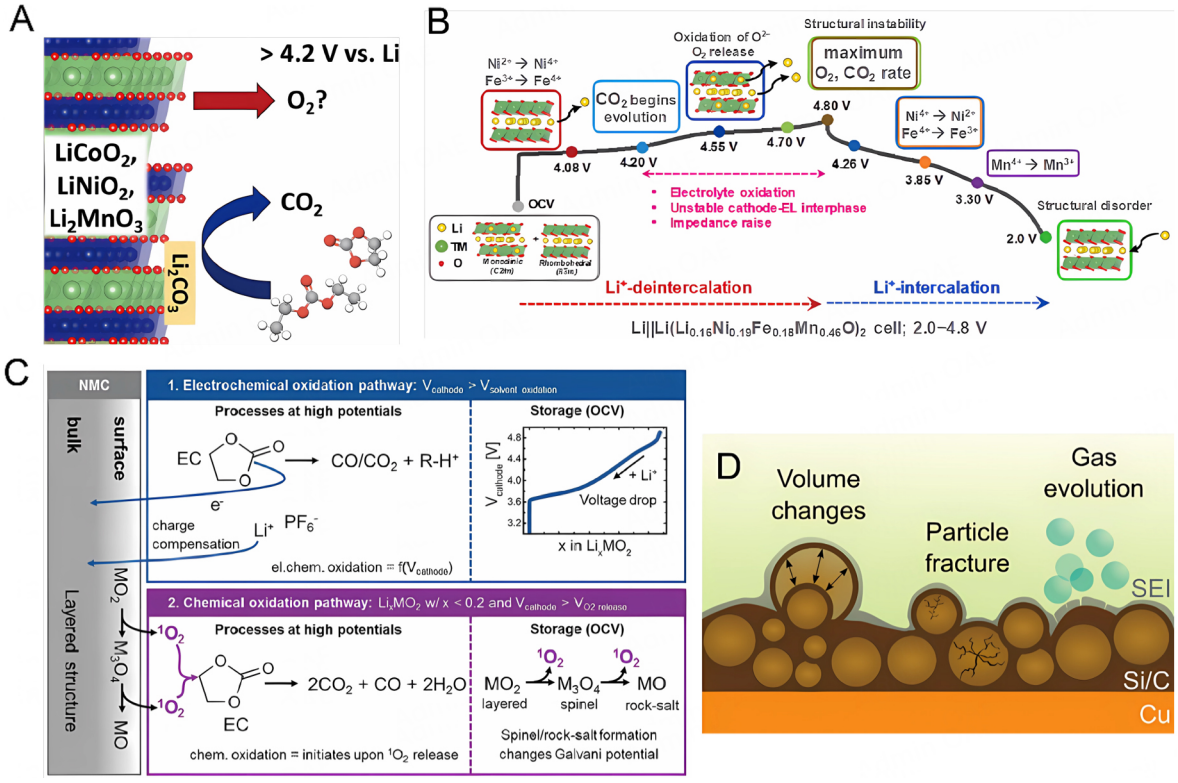

Figure 6. Gas evolution in lithium-ion batteries (LIBs). (A) Release of O_2 and CO_2 from layered transition metal oxide cathodes[119]. Copyright 2021, Elsevier. (B) Structural evolution, gas generation, and interface reactions during high-voltage charging of lithium-rich and manganese-rich layered oxide cathodes[126]. Copyright 2022, Elsevier. (C) Schematic description of the proposed electrochemical and chemical electrolyte oxidation pathways (exemplarily shown for EC)[37]. Copyright 2017, IOP Publishing. (D) Suppression of gas generation and particle fracture with carbon-coated silicon nanoparticles[138]. Copyright 2018, American Chemical Society.

flammable gases (hydrogen, ethylene [C_2H_4), and propylene], leading to thermal runaway of the battery. In QSEs, under high voltage, EC undergoes electron transfer at the negative electrode, resulting in the electrochemical reduction and generation of lithium ethylene dicarbonate (LEDC), C_2H_4, and CO[131]. As shown in Figure 6C, C_2H_4 production on graphite surfaces can be attributed to electrolyte reduction at 0.8 V[132]: $2EC + 2Li^+ + 2e^- \rightarrow C_2H_4 + (CH_2OCO_2Li)_2$ and $EC + 2Li^+ + 2e^- \rightarrow C_2H_4 + Li_2CO_3$. Other solvents, such as EMC, contribute to CO production, while PC-based electrolytes facilitate the production of CO_2, CO, and C_3H_8/C_3H_6[133]. DMC solvent promotes CH_4 generation. Additionally, the choice of salt significantly influences gas generation; for example, lithium bis(oxalato)borate (LiBOB)-based electrolytes undergo decomposition reactions under overcharge conditions, reacting with highly active oxygen released from the positive electrode material to produce CO_2. PEs can suppress interfacial reactions between the electrolyte and electrode and gas generation[134].

Electrode surface coatings and artificial SEI layers can passivate the electrode surface. For instance, carbon [Figure 6D], ceramic[135], and atomic layer deposition coatings[136] inhibit gas generation while maintaining high ionic conductivity[137]. Using antioxidant polymers at the positive electrode and anti-reductive polymers at the negative electrode can mitigate secondary reactions at the battery interfaces, ensuring high-voltage operation of the battery. Furthermore, the design of PE compositions facilitates the formation of stable SEI layers on electrode surfaces, suppressing parasitic reactions and addressing gas generation issues[138]. To avoid continuous formation and dissolution of SEI layers, electrolyte components used for SEI formation should prioritize reduction or oxidation (with low LUMO and high HOMO). Electrolyte

structure design is often employed to suppress interface reactions (including high-concentration electrolytes) to broaden the ESW and inhibit gas generation in high-concentration or locally concentrated electrolytes[139].

CONCLUSIONS AND OUTLOOK

This article reviews the research progress and challenges of PEs for high-voltage solid-state batteries. PEs need to simultaneously have broad ESW and compatibility with electrode interfaces. The high-voltage compatibility can be achieved by designing layered composite structures or interface passivation. Developing GPEs is an effective approach to addressing challenges electrolytes face under high and low temperature conditions (such as low electrochemical stability, interface degradation, electrolyte decomposition, *etc*.). Nonetheless, there are many aspects to be improved for high-voltage PEs, with potential solutions being detailed below:

(1) Intrinsic stability of polymer-based solid electrolytes. Intrinsic stability refers to the minimal occurrence of electrolyte decomposition reactions between polymer-based solid electrolytes and electrodes under high voltages. In polymer systems, matrices with electron-withdrawing groups generally exhibit higher stability. Therefore, strategies such as designing the polymer molecular structure, grafting electron-withdrawing groups, and increasing the degree of polymer crosslinking hold potential for stabilizing electrolytes under high-voltage conditions.

(2) Non-intrinsic stability of polymer-based solid electrolytes. For polymer-based solid electrolytes inherently unstable under high voltages, non-intrinsic high-voltage stability can be achieved by designing interface passivation layers and implementing composite electrolyte strategies. (1) The interface passivation layers can generate an ideal interfacial phase with high ionic conductivity and low electronic conductivity, dynamically suppressing electrochemical decomposition and facilitating stable operation of batteries under high voltages; and (2) constructing composite electrolytes regulates local molecular interactions, thereby delaying the high-voltage decomposition of solid electrolytes.

(3) Advanced characterization techniques and theoretical computations. Currently, solid electrolytes and the electrode/electrolyte interfaces in solid-state systems remain shrouded in mystery. Combining *in-situ* observations and multiscale calculations makes it possible to elucidate the interactions among polymer chains, small molecules, and ions in the system, guiding the design of novel polymer-based solid electrolytes. Additionally, advanced techniques are employed to track interface evolution and characterize interfaces under high voltages. This enables a more detailed investigation of interface reactions, ion transport across multiphase interfaces, and other complex interface behaviors.

(4) Developments of polymer-based electrolytes with high anodic stability are highly desired for enhancing the energy density of lithium batteries. The engineering parameters, such as thin electrolytes, high-loading cathodes, and suitable Negative/Positive capacity (N/P) ratios, are very important to achieve high energy density; the electrochemical performance of high-voltage batteries with the combination of these parameters is suggested to be further explored.

Therefore, the following research proposals are made for PE: For polymers such as PAN and PVDF that are compatible with 5 V-level high-voltage cathode materials, improving their negative electrode stability and room-temperature ionic conductivity are key for future research. For SPEs, reducing electrolyte thickness while ensuring mechanical performance can compensate for the low ionic conductivity, thereby enhancing rate capability and reducing the operating temperature of solid-state lithium batteries. Additionally, ceramic

particle dispersing, plasticizer addition, and liquid solvent incorporation all contribute to enhancing their room temperature performance.

GPEs simultaneously address issues of low ionic conductivity and electrode-electrolyte interface contacts. Future research on GPEs will primarily focus on improving safety and reducing liquid content. For instance, polymer grafting or copolymerization with halogen and phosphate-based monomers can eliminate radicals during battery ignition, thereby achieving flame-retardant effects. Importantly, GPEs can be adapted to existing liquid battery production lines, significantly reducing production complexity and cost. Transitioning from quasi-solid-state to all-solid-state polymer batteries will gradually eliminate flammable liquid batteries, enhancing the battery safety.

DECLARATIONS

Authors' contributions

Proposed the topic of this review: Fu J
Prepared the manuscript: Wang Z, Chen J
Collectively discussed and revised the manuscript: Wang Z, Chen J, Fu J, Li Z, Guo X

Availability of data and materials

Not applicable.

Financial support and sponsorship

This work was supported by the Natural Science Foundation of Hubei Province, China (Grant No. 2022CFA031) and Dongguan Innovative Research Team Program (2020607101007).

Conflicts of interest

All authors declared that there are no conflicts of interest.

Ethical approval and consent to participate

Not applicable.

Consent for publication

Not applicable.

REFERENCES

1. Gao Y, Jiang J, Zhang C, Zhang W, Ma Z, Jiang Y. Lithium-ion battery aging mechanisms and life model under different charging stresses. *J Power Sources* 2017;356:103-14. DOI
2. Zhou J, Qian T, Liu J, Wang M, Zhang L, Yan C. High-safety all-solid-state lithium-metal battery with high-ionic-conductivity thermoresponsive solid polymer electrolyte. *Nano Lett* 2019;19:3066-73. DOI
3. Zhao Q, Liu X, Stalin S, Khan K, Archer LA. Solid-state polymer electrolytes with in-built fast interfacial transport for secondary lithium batteries. *Nat Energy* 2019;4:365-73. DOI
4. Liu N, Lu Z, Zhao J, et al. A pomegranate-inspired nanoscale design for large-volume-change lithium battery anodes. *Nat Nanotechnol* 2014;9:187-92. DOI
5. Jung JW, Ryu WH, Shin J, Park K, Kim ID. Glassy metal alloy nanofiber anodes employing graphene wrapping layer: toward ultralong-cycle-life lithium-ion batteries. *ACS Nano* 2015;9:6717-27. DOI PubMed
6. Li J, Ma C, Chi M, Liang C, Dudney NJ. Solid electrolyte: the key for high-voltage lithium batteries. *Adv Energy Mater* 2015;5:1401408. DOI
7. Janek J, Zeier WG. A solid future for battery development. *Nat Energy* 2016;1:16141. DOI

8. Manthiram A, Yu X, Wang S. Lithium battery chemistries enabled by solid-state electrolytes. *Nat Rev Mater* 2017;2:16103. DOI
9. Wright PV. Electrical conductivity in ionic complexes of poly(ethylene oxide). *Brit Poly J* 1975;7:319-27. DOI
10. Fenton D, Parker J, Wright P. Complexes of alkali metal ions with poly(ethylene oxide). *Polymer* 1973;14:589. DOI
11. Armand M. Polymer solid electrolytes - an overview. *Solid State Ion* 1983;9-10:745-54. DOI
12. Sun C, Liu J, Gong Y, Wilkinson DP, Zhang J. Recent advances in all-solid-state rechargeable lithium batteries. *Nano Energy* 2017;33:363-86. DOI
13. Feuillade G, Perche P. Ion-conductive macromolecular gels and membranes for solid lithium cells. *J Appl Electrochem* 1975;5:63-9. DOI
14. Song J, Wang Y, Wan C. Review of gel-type polymer electrolytes for lithium-ion batteries. *J Power Sources* 1999;77:183-97. DOI
15. Cheng X, Pan J, Zhao Y, Liao M, Peng H. Gel polymer electrolytes for electrochemical energy storage. *Adv Energy Mater* 2018;8:1702184. DOI
16. Ren W, Ding C, Fu X, Huang Y. Advanced gel polymer electrolytes for safe and durable lithium metal batteries: challenges, strategies, and perspectives. *Energy Stor Mater* 2021;34:515-35. DOI
17. Chen S, Wen K, Fan J, Bando Y, Golberg D. Progress and future prospects of high-voltage and high-safety electrolytes in advanced lithium batteries: from liquid to solid electrolytes. *J Mater Chem A* 2018;6:11631-63. DOI
18. Xu L, Tang S, Cheng Y, et al. Interfaces in solid-state lithium batteries. *Joule* 2018;2:1991-2015. DOI
19. Weston J, Steele B. Effects of inert fillers on the mechanical and electrochemical properties of lithium salt-poly(ethylene oxide) polymer electrolytes. *Solid State Ion* 1982;7:75-9. DOI
20. Croce F, Appetecchi GB, Persi L, Scrosati B. Nanocomposite polymer electrolytes for lithium batteries. *Nature* 1998;394:456-8. DOI
21. Yue L, Ma J, Zhang J, et al. All solid-state polymer electrolytes for high-performance lithium ion batteries. *Energy Stor Mater* 2016;5:139-64. DOI
22. Yoshida K, Nakamura M, Kazue Y, et al. Oxidative-stability enhancement and charge transport mechanism in glyme-lithium salt equimolar complexes. *J Am Chem Soc* 2011;133:13121-9. DOI
23. Wetjen M, Kim G, Joost M, Appetecchi GB, Winter M, Passerini S. Thermal and electrochemical properties of PEO-LiTFSI-Pyr14TFSI-based composite cathodes, incorporating 4 V-class cathode active materials. *J Power Sources* 2014;246:846-57. DOI
24. Nie K, Wang X, Qiu J, et al. Increasing poly(ethylene oxide) stability to 4.5 V by surface coating of the cathode. *ACS Energy Lett* 2020;5:826-32. DOI
25. Yang X, Jiang M, Gao X, et al. Determining the limiting factor of the electrochemical stability window for PEO-based solid polymer electrolytes: main chain or terminal -OH group? *Energy Environ Sci* 2020;13:1318-25. DOI
26. Pandian S, Adiga S, Tagade P, Hariharan K, Mayya K, Lee Y. Electrochemical stability of ether based salt-in-polymer based electrolytes: computational investigation of the effect of substitution and the type of salt. *J Power Sources* 2018;393:204-10. DOI
27. Zhang Z, Hu L, Wu H, et al. Fluorinated electrolytes for 5 V lithium-ion battery chemistry. *Energy Environ Sci* 2013;6:1806-10. DOI
28. Sun H, Xie X, Huang Q, et al. Fluorinated poly-oxalate electrolytes stabilizing both anode and cathode interfaces for all-solid-state Li/NMC811 batteries. *Angew Chem Int Ed* 2021;60:18335-43. DOI
29. Xie X, Wang Z, He S, et al. Influencing factors on Li-ion conductivity and interfacial stability of solid polymer electrolytes, exampled by polycarbonates, polyoxalates and polymalonates. *Angew Chem Int Ed* 2023;62:e202218229. DOI
30. Tang L, Chen B, Zhang Z, et al. Polyfluorinated crosslinker-based solid polymer electrolytes for long-cycling 4.5 V lithium metal batteries. *Nat Commun* 2023;14:2301. DOI PubMed PMC
31. Lv Z, Zhou Q, Zhang S, et al. Cyano-reinforced in-situ polymer electrolyte enabling long-life cycling for high-voltage lithium metal batteries. *Energy Stor Mater* 2021;37:215-23. DOI
32. Dong T, Zhang H, Hu R, et al. A rigid-flexible coupling poly(vinylene carbonate) based cross-linked network: a versatile polymer platform for solid-state polymer lithium batteries. *Energy Stor Mater* 2022;50:525-32. DOI
33. Li S, Zhang SQ, Shen L, et al. Progress and perspective of ceramic/polymer composite solid electrolytes for lithium batteries. *Adv Sci* 2020;7:1903088. DOI PubMed PMC
34. Meng N, Zhu X, Lian F. Particles in composite polymer electrolyte for solid-state lithium batteries: a review. *Particuology* 2022;60:14-36. DOI
35. Pan J, Zhao P, Wang N, Huang F, Dou S. Research progress in stable interfacial constructions between composite polymer electrolytes and electrodes. *Energy Environ Sci* 2022;15:2753-75. DOI
36. Zhu Y, Cao J, Chen H, Yu Q, Li B. High electrochemical stability of a 3D cross-linked network PEO@nano-SiO_2 composite polymer electrolyte for lithium metal batteries. *J Mater Chem A* 2019;7:6832-9. DOI
37. Yu J, Wang C, Li S, Liu N, Zhu J, Lu Z. Li^+-containing, continuous silica nanofibers for high Li^+ conductivity in composite polymer electrolyte. *Small* 2019;15:e1902729. DOI
38. Huang H, Ding F, Zhong H, et al. Nano-SiO_2-embedded poly(propylene carbonate)-based composite gel polymer electrolyte for lithium-sulfur batteries. *J Mater Chem A* 2018;6:9539-49. DOI
39. Zhao XG, Jin EM, Park J, Gu H. Hybrid polymer electrolyte composite with SiO_2 nanofiber filler for solid-state dye-sensitized solar cells. *Compos Sci Technol* 2014;103:100-5. DOI
40. Zhai H, Gong T, Xu B, et al. Stabilizing polyether electrolyte with a 4 V metal oxide cathode by nanoscale interfacial coating. *ACS Appl Mater Interfaces* 2019;11:28774-80. DOI

41. Arya A, Sharma AL. Structural, microstructural and electrochemical properties of dispersed-type polymer nanocomposite films. *J Phys D Appl Phys* 2018;51:045504. DOI
42. Cao J, Wang L, He X, et al. *In situ* prepared nano-crystalline TiO_2-poly(methyl methacrylate) hybrid enhanced composite polymer electrolyte for Li-ion batteries. *J Mater Chem A* 2013;1:5955-61. DOI
43. Masoud EM, El-bellihi A, Bayoumy WA, Mohamed EA. Polymer composite containing nano magnesium oxide filler and lithiumtriflate salt: an efficient polymer electrolyte for lithium ion batteries application. *J Mol Liq* 2018;260:237-44. DOI
44. Dhatarwal P, Choudhary S, Sengwa R. Electrochemical performance of Li^+-ion conducting solid polymer electrolytes based on PEO-PMMA blend matrix incorporated with various inorganic nanoparticles for the lithium ion batteries. *Compos Commun* 2018;10:11-7. DOI
45. Lv F, Wang Z, Shi L, et al. Challenges and development of composite solid-state electrolytes for high-performance lithium ion batteries. *J Power Sources* 2019;441:227175. DOI
46. Zhou Q, Ma J, Dong S, Li X, Cui G. Intermolecular chemistry in solid polymer electrolytes for high-energy-density lithium batteries. *Adv Mater* 2019;31:e1902029. DOI
47. Wang Z, Huang X, Chen L. Understanding of effects of nano-Al_2O_3 particles on ionic conductivity of composite polymer electrolytes. *Electrochem Solid State Lett* 2003;6:E40. DOI
48. Wang Y, Wu L, Lin Z, et al. Hydrogen bonds enhanced composite polymer electrolyte for high-voltage cathode of solid-state lithium battery. *Nano Energy* 2022;96:107105. DOI
49. Yang H, Zhang B, Jing M, et al. In situ catalytic polymerization of a highly homogeneous PDOL composite electrolyte for long-cycle high-voltage solid-state lithium batteries (Adv. Energy Mater. 39/2022). *Adv Energy Mater* 2022;12:2201762. DOI
50. Fu K, Gong Y, Hitz GT, et al. Three-dimensional bilayer garnet solid electrolyte based high energy density lithium metal-sulfur batteries. *Energy Environ Sci* 2017;10:1568-75. DOI
51. Xie H, Yang C, Fu K, et al. Flexible, scalable, and highly conductive garnet-polymer solid electrolyte templated by bacterial cellulose. *Adv Energy Mater* 2018;8:1703474. DOI
52. Bae J, Li Y, Zhang J, et al. A 3D nanostructured hydrogel-framework-derived high-performance composite polymer lithium-ion electrolyte. *Angew Chem Int Ed* 2018;57:2096-100. DOI
53. Liu S, Liu W, Ba D, et al. Filler-integrated composite polymer electrolyte for solid-state lithium batteries. *Adv Mater* 2023;35:e2110423. DOI
54. Xu R, Xiao Y, Zhang R, et al. Dual-phase single-ion pathway interfaces for robust lithium metal in working batteries. *Adv Mater* 2019;31:e1808392. DOI
55. Li Y, Xu B, Xu H, et al. Hybrid polymer/garnet electrolyte with a small interfacial resistance for lithium-ion batteries. *Angew Chem Int Ed* 2017;56:753-6. DOI
56. Choi J, Lee C, Yu J, Doh C, Lee S. Enhancement of ionic conductivity of composite membranes for all-solid-state lithium rechargeable batteries incorporating tetragonal $Li_7La_3Zr_2O_{12}$ into a polyethylene oxide matrix. *J Power Sources* 2015;274:458-63. DOI
57. Cai D, Qi X, Xiang J, et al. A cleverly designed asymmetrical composite electrolyte via in-situ polymerization for high-performance, dendrite-free solid state lithium metal battery. *Chem Eng J* 2022;435:135030. DOI
58. Reddy MV, Julien CM, Mauger A, Zaghib K. Sulfide and oxide inorganic solid electrolytes for all-solid-state li batteries: a review. *Nanomaterials* 2020;10:1606. DOI PubMed PMC
59. Xu H, Chien PH, Shi J, et al. High-performance all-solid-state batteries enabled by salt bonding to perovskite in poly(ethylene oxide). *Proc Natl Acad Sci USA* 2019;116:18815-21. DOI PubMed PMC
60. Ma C, Cui W, Liu X, Ding Y, Wang Y. In situ preparation of gel polymer electrolyte for lithium batteries: progress and perspectives. *InfoMat* 2022;4:e12232. DOI
61. Zhu Y, Xiao S, Shi Y, Yang Y, Hou Y, Wu Y. A composite gel polymer electrolyte with high performance based on poly(vinylidene fluoride) and polyborate for lithium ion batteries. *Adv Energy Mater* 2014;4:1300647. DOI
62. Zhou D, Shanmukaraj D, Tkacheva A, Armand M, Wang G. Polymer electrolytes for lithium-based batteries: advances and prospects. *Chem* 2019;5:2326-52. DOI
63. Li G, Li Z, Zhang P, Zhang H, Wu Y. Research on a gel polymer electrolyte for Li-ion batteries. *Pure Appl Chem* 2008;80:2553-63. DOI
64. Sun Q, Wang S, Ma Y, et al. Li-ion transfer mechanism of gel polymer electrolyte with sole fluoroethylene carbonate solvent. *Adv Mater* 2023;35:e2300998. DOI
65. Chen M, Ma C, Ding Z, et al. Upgrading electrode/electrolyte interphases via polyamide-based quasi-solid electrolyte for long-life nickel-rich lithium metal batteries. *ACS Energy Lett* 2021;6:1280-9. DOI
66. Zeng Y, Yang J, Shen X, et al. New UV-initiated lithiated-interpenetrating network gel-polymer electrolytes for lithium-metal batteries. *J Power Sources* 2022;541:231681. DOI
67. Gao X, Yuan W, Yang Y, et al. High-performance and highly safe solvate ionic liquid-based gel polymer electrolyte by rapid UV-curing for lithium-ion batteries. *ACS Appl Mater Interfaces* 2022;14:43397-406. DOI
68. Li S, Sun Y, Li N, et al. Porosity development at Li-rich layered cathodes in all-solid-state battery during in situ delithiation. *Nano Lett* 2022;22:4905-11. DOI
69. Wang L, Xie R, Chen B, et al. In-situ visualization of the space-charge-layer effect on interfacial lithium-ion transport in all-solid-

state batteries. *Nat Commun* 2020;11:5889. DOI PubMed PMC

70. Koerver R, Walther F, Aygün I, et al. Redox-active cathode interphases in solid-state batteries. *J Mater Chem A* 2017;5:22750-60. DOI
71. Koerver R, Aygün I, Leichtweiß T, et al. Capacity fade in solid-state batteries: interphase formation and chemomechanical processes in nickel-rich layered oxide cathodes and lithium thiophosphate solid electrolytes. *Chem Mater* 2017;29:5574-82. DOI
72. Zhao CZ, Zhao Q, Liu X, et al. Rechargeable lithium metal batteries with an in-built solid-state polymer electrolyte and a high voltage/loading Ni-rich layered cathode. *Adv Mater* 2020;32:e1905629. DOI
73. Yan Y, Ju J, Dong S, et al. In situ polymerization permeated three-dimensional Li^+-percolated porous oxide ceramic framework boosting all solid-state lithium metal battery. *Adv Sci* 2021;8:2003887. DOI PubMed PMC
74. Li Z, Zhou X, Guo X. High-performance lithium metal batteries with ultraconformal interfacial contacts of quasi-solid electrolyte to electrodes. *Energy Stor Mater* 2020;29:149-55. DOI
75. Lu X, Daemi SR, Bertei A, et al. Microstructural evolution of battery electrodes during calendering. *Joule* 2020;4:2746-68. DOI
76. Judez X, Eshetu GG, Li C, Rodriguez-Martinez LM, Zhang H, Armand M. Opportunities for rechargeable solid-state batteries based on Li-intercalation cathodes. *Joule* 2018;2:2208-24. DOI
77. Zhao Q, Chen P, Li S, Liu X, Archer LA. Solid-state polymer electrolytes stabilized by task-specific salt additives. *J Mater Chem A* 2019;7:7823-30. DOI
78. Besli MM, Xia S, Kuppan S, et al. Mesoscale chemomechanical interplay of the $LiNi_{0.8}Co_{0.15}Al_{0.05}O_2$ cathode in solid-state polymer batteries. *Chem Mater* 2019;31:491-501. DOI
79. Lu X, Bertei A, Finegan DP, et al. 3D microstructure design of lithium-ion battery electrodes assisted by X-ray nano-computed tomography and modelling. *Nat Commun* 2020;11:2079. DOI PubMed PMC
80. Yang L, Zhang J, Xue W, et al. Anomalous thermal decomposition behavior of polycrystalline $LiNi_{0.8}Mn_{0.1}Co_{0.1}O_2$ in PEO-based solid polymer electrolyte. *Adv Funct Mater* 2022;32:2200096. DOI
81. Zhu GR, Zhang Q, Liu QS, et al. Non-flammable solvent-free liquid polymer electrolyte for lithium metal batteries. *Nat Commun* 2023;14:4617. DOI PubMed PMC
82. An H, Liu Q, Deng B, et al. Eliminating local electrolyte failure induced by asynchronous reaction for high-loading and long-lifespan all-solid-state batteries. *Adv Funct Mater* 2023;33:2305186. DOI
83. Liu Y, Liu H, Lin Y, et al. Mechanistic investigation of polymer-based all-solid-state lithium/sulfur battery. *Adv Funct Mater* 2021;31:2104863. DOI
84. Wang L, Zhang X, Wang T, et al. Ameliorating the interfacial problems of cathode and solid-state electrolytes by interface modification of functional polymers. *Adv Energy Mater* 2018;8:1801528. DOI
85. Liang L, Yuan W, Chen X, Liao H. Flexible, nonflammable, highly conductive and high-safety double cross-linked poly(ionic liquid) as quasi-solid electrolyte for high performance lithium-ion batteries. *Chem Eng J* 2021;421:130000. DOI
86. Didwal PN, Verma R, Nguyen AG, Ramasamy HV, Lee GH, Park CJ. Improving cyclability of all-solid-state batteries via stabilized electrolyte-electrode interface with additive in poly(propylene carbonate) based solid electrolyte. *Adv Sci* 2022;9:e2105448. DOI PubMed PMC
87. Chen Y, Cui Y, Wang S, et al. Durable and adjustable interfacial engineering of polymeric electrolytes for both stable Ni-rich cathodes and high-energy metal anodes. *Adv Mater* 2023;35:e2300982. DOI
88. Ni L, Zhang S, Di A, et al. Challenges and strategies towards single-crystalline Ni-rich layered cathodes. *Adv Energy Mater* 2022;12:2201510. DOI
89. Liu K, Pei A, Lee HR, et al. Lithium metal anodes with an adaptive "solid-liquid" interfacial protective layer. *J Am Chem Soc* 2017;139:4815-20. DOI
90. Yu X, Wang L, Ma J, Sun X, Zhou X, Cui G. Selectively wetted rigid-flexible coupling polymer electrolyte enabling superior stability and compatibility of high-voltage lithium metal batteries. *Adv Energy Mater* 2020;10:1903939. DOI
91. Ding P, Wu L, Lin Z, et al. Molecular self-assembled ether-based polyrotaxane solid electrolyte for lithium metal batteries. *J Am Chem Soc* 2023;145:1548-56. DOI
92. Li X, Lv M, Tian Y, et al. Negatively charged polymeric interphase for regulated uniform lithium-ion transport in stable lithium metal batteries. *Nano Energy* 2021;87:106214. DOI
93. Zhou T, Zhao Y, Choi JW, Coskun A. Ionic liquid functionalized gel polymer electrolytes for stable lithium metal batteries. *Angew Chem Int Ed* 2021;60:22791-6. DOI PubMed PMC
94. Chen N, Dai Y, Xing Y, et al. Biomimetic ant-nest ionogel electrolyte boosts the performance of dendrite-free lithium batteries. *Energy Environ Sci* 2017;10:1660-7. DOI
95. Lu Y, Zhao C, Yuan H, Cheng X, Huang J, Zhang Q. Critical current density in solid-state lithium metal batteries: mechanism, influences, and strategies. *Adv Funct Mater* 2021;31:2009925. DOI
96. Kim J, Ma H, Cha H, et al. A highly stabilized nickel-rich cathode material by nanoscale epitaxy control for high-energy lithium-ion batteries. *Energy Environ Sci* 2018;11:1449-59. DOI
97. Wang H, Zhu QL, Zou R, Xu Q. Metal-organic frameworks for energy applications. *Chem* 2017;2:52-80. DOI
98. Qian J, Li Y, Zhang M, et al. Protecting lithium/sodium metal anode with metal-organic framework based compact and robust shield. *Nano Energy* 2019;60:866-74. DOI
99. Huo H, Wu B, Zhang T, et al. Anion-immobilized polymer electrolyte achieved by cationic metal-organic framework filler for

dendrite-free solid-state batteries. *Energy Stor Mater* 2019;18:59-67. DOI

100. Cui S, Wu X, Yang Y, et al. Heterostructured gel polymer electrolyte enabling long-cycle quasi-solid-state lithium metal batteries. *ACS Energy Lett* 2022;7:42-52. DOI
101. Ma Q, Fu S, Wu A, et al. Designing bidirectionally functional polymer electrolytes for stable solid lithium metal batteries. *Adv Energy Mater* 2023;13:2203892. DOI
102. Yang F, Liu Y, Liu T, et al. Fluorinated strategies among all-solid-state lithium metal batteries from microperspective. *Small Struct* 2023;4:2200122. DOI
103. Qi S, Li M, Gao Y, et al. Enabling scalable polymer electrolyte with dual-reinforced stable interface for 4.5 V lithium-metal batteries. *Adv Mater* 2023;35:e2304951. DOI
104. Liu FQ, Wang WP, Yin YX, et al. Upgrading traditional liquid electrolyte via in situ gelation for future lithium metal batteries. *Sci Adv* 2018;4:eaat5383. DOI PubMed PMC
105. Lou S, Liu Q, Zhang F, et al. Insights into interfacial effect and local lithium-ion transport in polycrystalline cathodes of solid-state batteries. *Nat Commun* 2020;11:5700. DOI PubMed PMC
106. Zhang N, Deng T, Zhang S, et al. Critical review on low-temperature Li-ion/metal batteries. *Adv Mater* 2022;34:e2107899. DOI
107. Li Z, Yu R, Weng S, Zhang Q, Wang X, Guo X. Tailoring polymer electrolyte ionic conductivity for production of low- temperature operating quasi-all-solid-state lithium metal batteries. *Nat Commun* 2023;14:482. DOI PubMed PMC
108. Zhang D, Liu Z, Wu Y, et al. In situ construction a stable protective layer in polymer electrolyte for ultralong lifespan solid-state lithium metal batteries. *Adv Sci* 2022;9:e2104277. DOI PubMed PMC
109. Li T, Zhang X, Shi P, Zhang Q. Fluorinated solid-electrolyte interphase in high-voltage lithium metal batteries. *Joule* 2019;3:2647-61. DOI
110. Liang JY, Zhang XD, Zeng XX, et al. Enabling a durable electrochemical interface via an artificial amorphous cathode electrolyte interphase for hybrid solid/liquid lithium-metal batteries. *Angew Chem Int Ed* 2020;59:6585-9. DOI
111. An SJ, Li J, Daniel C, Mohanty D, Nagpure S, Wood DL. The state of understanding of the lithium-ion-battery graphite solid electrolyte interphase (SEI) and its relationship to formation cycling. *Carbon* 2016;105:52-76. DOI
112. Zhang Z, Li Y, Xu R, et al. Capturing the swelling of solid-electrolyte interphase in lithium metal batteries. *Science* 2022;375:66-70. DOI
113. Tu S, Zhang B, Zhang Y, et al. Fast-charging capability of graphite-based lithium-ion batteries enabled by Li_3P-based crystalline solid-electrolyte interphase. *Nat Energy* 2023;8:1365-74. DOI
114. Heiskanen SK, Kim J, Lucht BL. Generation and evolution of the solid electrolyte interphase of lithium-ion batteries. *Joule* 2019;3:2322-33. DOI
115. Dong H, Wang J, Wang V, et al. Effect of temperature on formation and evolution of solid electrolyte interphase on Si@Graphite@C anodes. *J Energy Chem* 2022;64:190-200. DOI
116. Rezqita A, Sauer M, Foelske A, Kronberger H, Trifonova A. The effect of electrolyte additives on electrochemical performance of silicon/mesoporous carbon (Si/MC) for anode materials for lithium-ion batteries. *Electrochim Acta* 2017;247:600-9. DOI
117. Kobayashi Y, Seki S, Mita Y, et al. High reversible capacities of graphite and SiO/graphite with solvent-free solid polymer electrolyte for lithium-ion batteries. *J Power Sources* 2008;185:542-8. DOI
118. Aiken CP, Self J, Petibon R, Xia X, Paulsen JM, Dahn JR. A survey of in situ gas evolution during high voltage formation in Li-ion pouch cells. *J Electrochem Soc* 2015;162:A760-7. DOI
119. Papp JK, Li N, Kaufman LA, et al. A comparison of high voltage outgassing of $LiCoO_2$, $LiNiO_2$, and Li_2MnO_3 layered Li-ion cathode materials. *Electrochim Acta* 2021;368:137505. DOI
120. Ren D, Feng X, Lu L, et al. An electrochemical-thermal coupled overcharge-to-thermal-runaway model for lithium ion battery. *J Power Sources* 2017;364:328-40. DOI
121. Browning KL, Baggetto L, Unocic RR, Dudney NJ, Veith GM. Gas evolution from cathode materials: a pathway to solvent decomposition concomitant to SEI formation. *J Power Sources* 2013;239:341-6. DOI
122. Han JG, Kim K, Lee Y, Choi NS. Scavenging materials to stabilize $LiPF_6$-containing carbonate-based electrolytes for Li-ion batteries. *Adv Mater* 2019;31:e1804822. DOI
123. Mahne N, Renfrew SE, McCloskey BD, Freunberger SA. Electrochemical oxidation of lithium carbonate generates singlet oxygen. *Angew Chem Int Ed* 2018;57:5529-33. DOI PubMed PMC
124. Zheng X, Li X, Wang Z, et al. Investigation and improvement on the electrochemical performance and storage characteristics of $LiNiO_2$-based materials for lithium ion battery. *Electrochim Acta* 2016;191:832-40. DOI
125. Jung R, Metzger M, Maglia F, Stinner C, Gasteiger HA. Oxygen release and its effect on the cycling stability of $LiNi_xMn_yCo_zO_2$ (NMC) cathode materials for Li-ion batteries. *J Electrochem Soc* 2017;164:A1361-77. DOI
126. Pham HQ, Kondracki Ł, Tarik M, Trabesinger S. Correlating the initial gas evolution and structural changes to cycling performance of Co-free Li-rich layered oxide cathode. *J Power Sources* 2022;527:231181. DOI
127. Fell CR, Sun L, Hallac PB, Metz B, Sisk B. Investigation of the gas generation in lithium titanate anode based lithium ion batteries. *J Electrochem Soc* 2015;162:A1916-20. DOI
128. Kanamura K, Toriyama S, Shiraishi S, Takehara Z. Studies on electrochemical oxidation of nonaqueous electrolytes using in situ FTIR spectroscopy: I. The effect of type of electrode on on-set potential for electrochemical oxidation of propylene carbonate containing 1.0 mol dm^{-3}. *J Electrochem Soc* 1995;142:1383-9. DOI

129. Kim Y, Park H, Warner JH, Manthiram A. Unraveling the intricacies of residual lithium in high-Ni cathodes for lithium-ion batteries. *ACS Energy Lett* 2021;6:941-8. DOI
130. Jiao S, Ren X, Cao R, et al. Stable cycling of high-voltage lithium metal batteries in ether electrolytes. *Nat Energy* 2018;3:739-46. DOI
131. Jung R, Metzger M, Maglia F, Stinner C, Gasteiger HA. Chemical versus electrochemical electrolyte oxidation on NMC111, NMC622, NMC811, LNMO, and conductive carbon. *J Phys Chem Lett* 2017;8:4820-5. DOI
132. Zhu Z, Wang H, Li Y, et al. A surface Se-substituted LiCo [$O_{2-\delta}Se_{\delta}$>] cathode with ultrastable high-voltage cycling in pouch full-cells. *Adv Mater* 2020;32:e2005182. DOI
133. Luo K, Roberts MR, Hao R, et al. Charge-compensation in 3D-transition-metal-oxide intercalation cathodes through the generation of localized electron holes on oxygen. *Nat Chem* 2016;8:684-91. DOI
134. Xu K. Electrolytes and interphases in Li-ion batteries and beyond. *Chem Rev* 2014;114:11503-618. DOI PubMed
135. Li W, Li X, Chen M, et al. AlF_3 modification to suppress the gas generation of $Li_4Ti_5O_{12}$ anode battery. *Electrochim Acta* 2014;139:104-10. DOI
136. Zhao K, Wang C, Yu Y, et al. Ultrathin surface coating enables stabilized zinc metal anode. *Adv Mater Inter* 2018;5:1800848. DOI
137. Zhang X, Belharouak I, Li L, et al. Structural and electrochemical study of Al_2O_3 and TiO_2 Coated $Li_{1.2}Ni_{0.13}Mn_{0.54}Co_{0.13}O_2$ cathode material using ALD. *Adv Energy Mater* 2013;3:1299-307. DOI
138. Schiele A, Breitung B, Mazilkin A, et al. Silicon nanoparticles with a polymer-derived carbon shell for improved lithium-ion batteries: investigation into volume expansion, gas evolution, and particle fracture. *ACS Omega* 2018;3:16706-13. DOI PubMed PMC
139. Tong X, Ou X, Wu N, Wang H, Li J, Tang Y. High oxidation potential ≈6.0 V of concentrated electrolyte toward high-performance dual-ion battery. *Adv Energy Mater* 2021;11:2100151. DOI
140. Chang C, Yao Y, Li R, et al. Self-healing single-ion-conductive artificial polymeric solid electrolyte interphases for stable lithium metal anodes. *Nano Energy* 2022;93:106871. DOI
141. Fu C, Homann G, Grissa R, et al. A polymerized-ionic-liquid-based polymer electrolyte with high oxidative stability for 4 and 5 V class solid-state lithium metal batteries. *Adv Energy Mater* 2022;12:2200412. DOI
142. Yao M, Ruan Q, Pan S, Zhang H, Zhang S. An ultrathin asymmetric solid polymer electrolyte with intensified ion transport regulated by biomimetic channels enabling wide-temperature high-voltage lithium-metal battery. *Adv Energy Mater* 2023;13:2203640. DOI
143. Li H, Du Y, Wu X, Xie J, Lian F. Developing "polymer-in-salt" high voltage electrolyte based on composite lithium salts for solid-state Li metal batteries. *Adv Funct Mater* 2021;31:2103049. DOI
144. Yao Z, Zhu K, Li X, et al. 3D poly(vinylidene fluoride-hexafluoropropylen) nanofiber-reinforced PEO-based composite polymer electrolyte for high-voltage lithium metal batteries. *Electrochim Acta* 2022;404:139769. DOI
145. Huang T, Xiong W, Ye X, et al. A cerium-doped NASICON chemically coupled poly(vinylidene fluoride-hexafluoropropylene)-based polymer electrolyte for high-rate and high-voltage quasi-solid-state lithium metal batteries. *J Energy Chem* 2022;73:311-21. DOI
146. Chen L, Gu T, Ma J, et al. In situ construction of Li_3N-enriched interface enabling ultra-stable solid-state $LiNi_{0.8}Co_{0.1}Mn_{0.1}O_2$/lithium metal batteries. *Nano Energy* 2022;100:107470. DOI
147. Ma X, Zuo X, Wu J, et al. Polyethylene-supported ultra-thin polyvinylidene fluoride/hydroxyethyl cellulose blended polymer electrolyte for 5 V high voltage lithium ion batteries. *J Mater Chem A* 2018;6:1496-503. DOI
148. Duan H, Fan M, Chen WP, et al. Extended electrochemical window of solid electrolytes via heterogeneous multilayered structure for high-voltage lithium metal batteries. *Adv Mater* 2019;31:e1807789. DOI
149. He F, Tang W, Zhang X, Deng L, Luo J. High energy density solid state lithium metal batteries enabled by Sub-5 µm solid polymer electrolytes. *Adv Mater* 2021;33:e2105329. DOI PubMed
150. Li J, Jing M, Li R, et al. Al_2O_3 fiber-reinforced polymer solid electrolyte films with excellent lithium-ion transport properties for high-voltage solid-state lithium batteries. *ACS Appl Polym Mater* 2022;4:7144-51. DOI
151. Zhu M, Wu J, Liu B, et al. Multifunctional polymer electrolyte improving stability of electrode-electrolyte interface in lithium metal battery under high voltage. *J Membr Sci* 2019;588:117194. DOI
152. Gong Y, Wang C, Xin M, et al. Ultra-thin and high-voltage-stable Bi-phasic solid polymer electrolytes for high-energy-density Li metal batteries. *Nano Energy* 2024;119:109054. DOI
153. Wang H, Song J, Zhang K, et al. A strongly complexed solid polymer electrolyte enables a stable solid state high-voltage lithium metal battery. *Energy Environ Sci* 2022;15:5149-58. DOI
154. Yang T, Zhang W, Lou J, et al. Stable LiF-rich electrode-electrolyte interface toward high-voltage and high-energy-density lithium metal solid batteries. *Small* 2023;19:e2300494. DOI
155. Wang Y, Chen S, Li Z, Peng C, Li Y, Feng W. In-situ generation of fluorinated polycarbonate copolymer solid electrolytes for high-voltage Li-metal batteries. *Energy Stor Mater* 2022;45:474-83. DOI
156. Yin X, Zhao S, Lin Z, et al. A propanesultone-based polymer electrolyte for high-energy solid-state lithium batteries with lithium-rich layered oxides. *J Mater Chem A* 2023;11:19118-27. DOI
157. Li Z, Fu J, Zheng S, Li D, Guo X. Self-healing polymer electrolyte for dendrite-free Li metal batteries with ultra-high-voltage Ni-rich layered cathodes. *Small* 2022;18:e2200891. DOI
158. Jing C, Dai K, Liu D, et al. Crosslinked solubilizer enables nitrate-enriched carbonate polymer electrolytes for stable, high-voltage

lithium metal batteries. *Sci Bull* 2024;69:209-17. DOI

159. Zhu J, Zhang J, Zhao R, et al. In situ 3D crosslinked gel polymer electrolyte for ultra-long cycling, high-voltage, and high-safety lithium metal batteries. *Energy Stor Mater* 2023;57:92-101. DOI
160. Zhou G, Yu J, Ciucci F. In situ prepared all-fluorinated polymer electrolyte for energy-dense high-voltage lithium-metal batteries. *Energy Stor Mater* 2023;55:642-51. DOI
161. Fang Z, Luo Y, Liu H, et al. Boosting the oxidative potential of polyethylene glycol-based polymer electrolyte to 4.36 V by Spatially restricting hydroxyl groups for high-voltage flexible lithium-ion battery applications. *Adv Sci* 2021;8:e2100736. DOI PubMed PMC
162. Zhu J, Zhao R, Zhang J, et al. Long-cycling and high-voltage solid state lithium metal batteries enabled by fluorinated and crosslinked polyether electrolytes. *Angew Chem Int Ed* 2024;63:e202400303. DOI
163. Wang A, Geng S, Zhao Z, Hu Z, Luo J. In situ cross-linked plastic crystal electrolytes for wide-temperature and high-energy-density lithium metal batteries. *Adv Funct Mater* 2022;32:2201861. DOI
164. Wang F, Liu H, Guo Y, et al. In situ high-performance gel polymer electrolyte with dual-reactive cross-linking for lithium metal batteries. *Energy Environ Mater* 2024;7:e12497. DOI
165. Wu J, Wang X, Liu Q, et al. A synergistic exploitation to produce high-voltage quasi-solid-state lithium metal batteries. *Nat Commun* 2021;12:5746. DOI PubMed PMC
166. Wang C, Liu H, Liang Y, et al. Molecular-level designed polymer electrolyte for high-voltage lithium-metal solid-state batteries. *Adv Funct Mater* 2023;33:2209828. DOI
167. Liu D, Lu Z, Lin Z, Zhang C, Dai K, Wei W. Organoboron- and cyano-grafted solid polymer electrolytes boost the cyclability and safety of high-voltage lithium metal batteries. *ACS Appl Mater Interfaces* 2023;15:21112-22. DOI
168. Hu R, Qiu H, Zhang H, et al. A polymer-reinforced SEI layer induced by a cyclic carbonate-based polymer electrolyte boosting 4.45 V $LiCoO_2$/Li metal batteries. *Small* 2020;16:e1907163. DOI
169. Dong T, Zhang J, Xu G, et al. A multifunctional polymer electrolyte enables ultra-long cycle-life in a high-voltage lithium metal battery. *Energy Environ Sci* 2018;11:1197-203. DOI
170. Liang JY, Zeng XX, Zhang XD, et al. Engineering janus interfaces of ceramic electrolyte via distinct functional polymers for stable high-voltage Li-metal batteries. *J Am Chem Soc* 2019;141:9165-9. DOI
171. Zhang H, Zhou L, Du X, et al. Cyanoethyl cellulose-based eutectogel electrolyte enabling high-voltage-tolerant and ion-conductive solid-state lithium metal batteries. *Carbon Energy* 2022;4:1093-106. DOI